Reaction kinetics and multi-sulfur products formation of sulfur-containing volatile organic compounds with OH radicals

Xun Rong[1], Lei Yao[1,2,3]*, Chuang Li[1], Cong An[1], Gan Yang[1], Jiali Shen[3], Runlong Cai[1,2], Douglas R. Worsnop[3,4], Lin Wang[1,2,3,6,7]

[1] Shanghai Key Laboratory of Air Quality and Environmental Health, Department of Environmental Science and Engineering, Jiangwan Campus, Fudan University, Shanghai 200438, China
[2] Shanghai Institute of Pollution Control and Ecological Security, Shanghai 200092, China
[3] National Observations and Research Station for Wetland Ecosystems of the Yangtze Estuary, Shanghai 200438, China
[4] Institute for Atmospheric and Earth System Research/Physics, Faculty of Science, University of Helsinki, 00014 Helsinki, Finland
[5] Aerodyne Research, Billerica, MA 01821, USA
[6] IRDR International Center of Excellence on Risk Interconnectivity and Governance on Weather/Climate Extremes Impact and Public Health, Fudan University, Shanghai 200438, China
[7] Collaborative Innovation Center of Climate Change, Nanjing, 210023, China

Correspondence: L.Y., email, lei_yao@fudan.edu.cn

Abstract. Atmospheric sulfur-containing volatile organic compounds (sulfur-VOCs) have been recognized as crucial precursors for gaseous sulfuric acid (H_2SO_4), particulate sulfate and secondary organic aerosol (SOA) formation. However, their reaction kinetics and multi-sulfur product formation remain poorly understood. This study presents a systematic kinetic investigation into •OH-initiated oxidation of a series of sulfur-VOCs including thiols and sulfides~~,~~. The reaction rate constants vary with molecular structure, with high reactivity observed for trimethylene sulfide and dimethyl disulfide.~~and the reaction rates of dithiols and cyclic sulfides are generally higher than that of monothiols and acyclic sulfides.~~ It was further demonstrated that under low NO_x, sulfur-containing RO_2 radicals can undergo bimolecular reactions forming low-volatility multi-sulfur products that enhance their SOA formation potential. Additionally, many sulfur-VOCs investigated in our chamber experiments are also identified from the emissions of algae samples collected from a major freshwater lake in China, and similar multi-sulfur oxidation products were observed after •OH oxidation. These findings advance the kinetic and mechanistic understanding of atmospheric sulfur-VOCs oxidation and suggest that the formation of low-volatility multi-sulfur products and inorganic sulfur-containing species may contribute to SOA production and new particle formation in marine and freshwater environments influenced by algal emissions.

Keywords: sulfur-VOCs, reaction rate constants~~rates~~, multi-sulfur products, freshwater algae

emissions, secondary organic aerosol

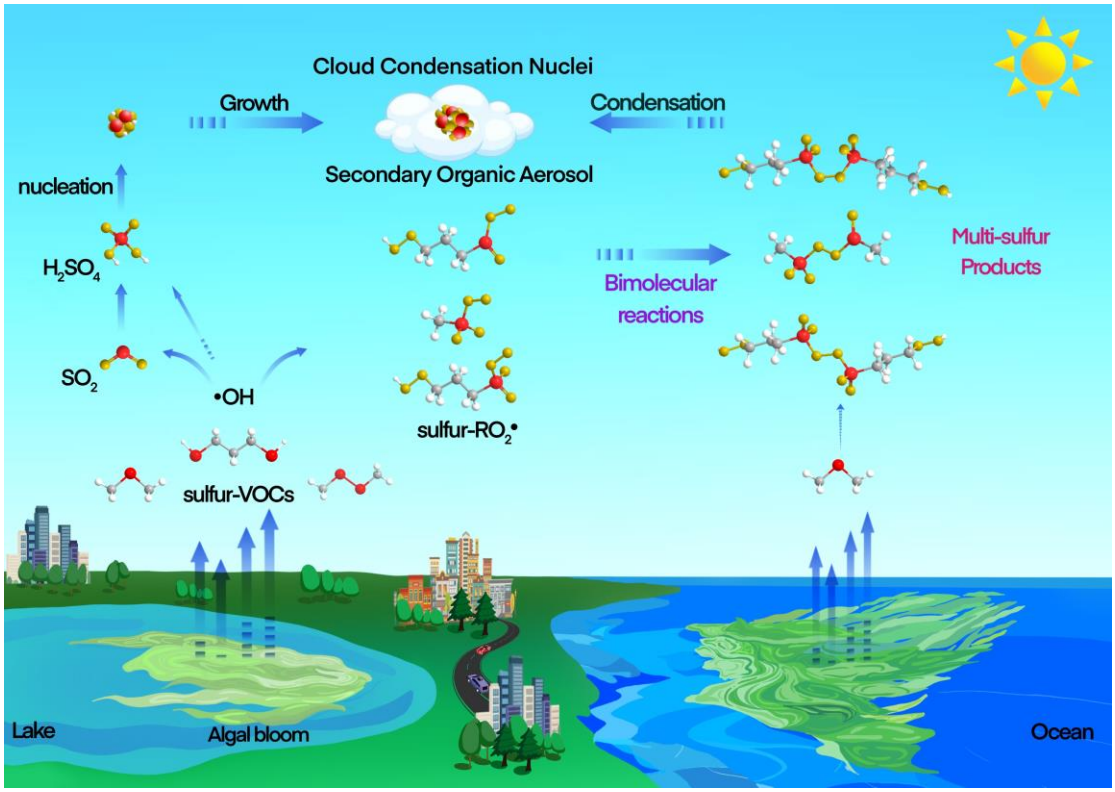

1 Introduction

Atmospheric sulfur-containing volatile organic compounds (sulfur-VOCs) (e.g., dimethyl sulfide (CH_3SCH_3, DMS), methanthiol (CH_3SH), dimethyl disulfide ($CH_3S_2CH_3$, DMDS), and carbonyl sulfide (OCS)) are important biogenic VOCs and mainly produced by degradation of sulfur-containing amino acids and methylation of sulfides (Kietäväinen et al., 2025; Kilgour et al., 2021; Li et al., 2022; Wang et al., 2023b). These compounds play a key role in the global atmospheric sulfur cycle, and their atmospheric oxidation products such as sulfuric acid (H_2SO_4) and methanesulfonic acid (CH_3SO_3H) are able to combine with basic species (e.g., NH_3 and amines) to form new particles and particulate sulfate , which can contribute to the formation of cloud condensation nuclei (CCN) and then have an effect on regional and global climate– (Bates et al., 1992; Charlson et al., 1987; Fiddes et al., 2021; Jokinen et al., 2022; Revell et al., 2024; Wang et al., 2023a).

At present, it is widely recognized that marine ecosystems (e.g., phytoplankton) are the dominant natural sources of atmospheric sulfur-VOCs, among which DMS is the dominate one and mainly produced via the dimethylsulfoniopropionate (DMSP) metabolic pathway of phytoplankton (Andreae and Raemdonck, 1983; Novak et al., 2022; Rocco et al., 2025). Foundational studies by Kiene and co-workers demonstrated that DMSP can be transformed in marine systems through microbial cleavage and demethylation pathways, leading to the formation of reduced sulfur compounds such as DMS and methanethiol (Kiene, 1996; Kiene et al., 2000; Kiene and Taylor, 1988; Kiene and Service, 1991; Visscher et al., 1994; Yoch, 2002). The importance of this source is further underscored by recent satellite-based observations showing that, between 2003 and 2020, the global spatial extent of coastal phytoplankton blooms expanded by 13.2% (+ 3.97 million km^2) and their frequency increased by 59.2%, indicating an overall intensification of marine algae activity (Dai et al., 2023). The measurements in marine boundary layer reported DMS mixing ratios ranging from tens to a few hundred pptv with pronounced seasonal maxima in biologically productive waters (Zhao et al., 2021). Co-emitted methanthiol is also detected and generally ranged from ~10 to 250 pptv (Mynard et al., 2025; Novak et al., 2022; Rocco et al., 2025).

In addition to marine phytoplankton, freshwater algae are also recognized as important sources of atmospheric sulfur-VOCs, including DMS, DMDS, and dimethyl trisulfide ($CH_3S_3CH_3$, DMTS), which are released through amino acid degradation and methylation processes (Bao et al., 2024; Huang et al., 2018; Li et al., 2022). This source is becoming particularly relevant in eutrophic freshwater lakes experiencing frequent algal blooms. In China, around 85.4% of the 138 major freshwater lakes with their areas larger than 10 km^2 suffer from varying degrees of eutrophication (Wang et al., 2022). In such systems, concentrations of DMS, DMDS, and DMTS in the water column commonly reach the microgram per liter level (Bao et al., 2024; Huang et al., 2018; Lu et

al., 2012; Yu et al., 2019a). Supporting the potential for atmospheric release, previous laboratory and field studies have quantified sulfur-VOCs emission fluxes from freshwater lakes, showing that DMS can be emitted at rates of several μmol m^{-2} d^{-1}, with emission intensity strongly modulated by seasonality and trophic status of lakes (Li et al., 2022; Steinke et al., 2018). Many sulfur-VOCs have been directly observed in the atmosphere near an inland freshwater lake (Dianshan Lake, Shanghai) during winter-spring campaigns, with mixing ratios of DMS, methanthiol and DMDS can be up to 331.4 pptv, 183.8 pptv, and 153.6 pptv, respectively (Deng et al., 2025).

Once released into the atmosphere, sulfur-VOCs can undergo oxidation by multiple atmospheric oxidants, includinghydroxyl radicals (•OH), nitrate radicals (NO_3•), and ozone (O_3), with •OH typically acting as the dominant daytime oxidant and NO_3• becoming important during nighttime conditions (Atkinson and Arey, 2003; Barnes et al., 2006; Du et al., 2007; Stark et al., 2007). The reaction rate constants between a few sulfur-VOCs (e.g., methanethiol, DMS, and DMDS~~rapidly react with hydroxyl radicals (•OH). The reaction rates between a few sulfur-VOCs (e.g., methanethiol, DMS, and DMDS)~~ and •OH have been well-established, with k_{OH} values of ~3.3×10^{-11} cm^3 $molecule^{-1}$ s^{-1} for methanthiol, ~7.0×10^{-12} cm^3 $molecule^{-1}$ s^{-1} for DMS, and ~2.3×10^{-10} cm^3 $molecule^{-1}$ s^{-1} for DMDS, at 298 K, respectively (Abbatt et al., 1992; Barnes et al., 1986; Cruz-Torres and Galano, 2007; Hashemi et al., 2019; Atkinson et al., 2004). These reactions play a critical role in determining the atmospheric lifetimes and transformation pathways of these sulfur VOCs. There are significant differences in the reactivity of sulfur-VOCs with different functional groups towards •OH, with thiols and disulfides generally exhibiting higher reactivity than that of mono-sulfides (Abbatt et al., 1992; Cruz-Torres and Galano, 2007; Hashemi et al., 2019; Tahan and Shiroudi, 2020). However, systematic understanding of reaction kinetics of sulfur-VOCs with different functional groups towards •OH remains limited, particularly for sulfur-VOCs with complex molecular structures which are increasingly detected in field measurements. For instance, 1-propanethiol ($CH_3(CH_2)_2SH$), 2-propanethiol ($(CH_3)_2CHSH$), methyl propyl disulfide ($CH_3S_2(CH_2)_2CH_3$), diethyl disulfide ($CH_3CH_2S_2CH_2CH_3$), and isopropyl disulfide ($(CH_3)_2CHS_2CH(CH_3)_2$) have been detected from freshwater algae emissions, yet data on their reaction kinetics with •OH remain scarce (Liu et al., 2021; Yu et al., 2019b; Zhou et al., 2024). Therefore, it hinders accurate assessments of the chemical behavior and environmental impact of these biogenic sulfur-VOCs in the atmosphere, particularly in aquatic environments (e.g., huge freshwater lakes) where algae blooms frequently occur.

Previous studies on the reaction mechanisms between some sulfur-VOCs and •OH have established a relatively comprehensive framework, evolving from early kinetic and product studies to more recent investigations of detailed radical chemistry and autoxidation processes (Berndt et al., 2024; Goss and Kroll, 2023; Shen et al., 2022; Ye et al., 2022). The initial steps typically involve

the formation of sulfur-containing radicals (sulfur-R•) via H-extraction or •OH-addition, which then combine with O_2 to generate various sulfur-containing RO_2 radicals (sulfur-RO_2•) (Berndt et al., 2023; Goss and Kroll, 2023; Shen et al., 2022). Among these, sulfides primarily form α-carbon peroxy radicals (e.g., CH_3SCH_2OO•), while thiols and disulfides tend to generate sulfur-centered peroxy radicals (e.g., RSOO•) (Berndt et al., 2023; Goss and Kroll, 2023; Lily et al., 2023). Although the unimolecular reactions (e.g., H-migration) and bimolecular reaction pathways involving NO_x and HO_2• of these sulfur-RO_2• species have been investigated, the bimolecular reactions between sulfur-RO_2• and sulfur-R'O_2• remain poorly characterized (Berndt et al., 2023; Jernigan et al., 2022; Shen et al., 2022).

This study systematically investigated the reaction kinetics and multi-sulfur products formation of 11 sulfur-VOCs with •OH using a Teflon chamber together with a Vocus proton transfer reaction long-time-of-flight mass spectrometry (Vocus-PTR-LToF-MS, Tofwerk AG) and a nitrate-based chemical ionization long-time-of-flight mass spectrometry (nitrate-CI-LToF-MS, Aerodyne Research) (Ehn et al., 2014; Krechmer et al., 2018). To investigate the relationship between products formation~~the reaction rates~~ and their molecular structures, these 11 sulfur-VOCs were divided into 5 classes, which are monothiols (i.e., ethanethiol (C_2H_6S), 1-propanethiol (C_3H_8S), and 2-propanethiol (C_3H_8S)), dithiols (i.e., 1,2-ethanedithiol ($C_2H_6S_2$), and 1,3-propanedithiol ($C_3H_8S_2$)), acyclic sulfides (i.e., dimethyl sulfide (C_2H_6S), methyl ethyl sulfide (C_3H_8S), and bis(methylthio)methane ($C_3H_8S_2$)), cyclic sulfides (i.e., trimethylene sulfide (C_3H_6S), and 1,3-dithiolane ($C_3H_6S_2$)) and disulfides (dimethyl disulfide ($C_2H_6S_2$)) (Table 1). Moreover, the emitted VOCs from freshwater algae samples taken from a huge freshwater lake (i.e., Taihu lake, China) and their oxidation products by •OH were also investigated. Similar sulfur-VOCs and multi-sulfur products were also observed from VOCs emitted from freshwater algae samples and their oxidation products, which demonstrates the atmospheric relevance of our selected sulfur-VOCs and their atmospheric transformation mechanisms in our study.

2 Materials and methods

2.1 Chamber experiments of 11 sulfur-VOCs with •OH

The selected 11 high-purity (≥ 96%) sulfur-VOCs liquid standards (Sigma-Aldrich and Macklin) were listed in Table S1. These liquid standards were then used to generate individual sulfur-VOC standard gases with our laboratory partial-pressure gas mixing system (Li et al., 2025; Wang et al., 2020). The experimental setup is shown in Figure S1. A 0.53 m^3 polytetrafluoroethylene (FEP) chamber was employed to conduct atmospheric oxidation experiments of sulfur-VOCs with •OH. The experimental conditions including the initial mixing ratios of sulfur-VOCs, O_3 concentration, and relative humidity (RH), are summarized in Table 1. These experiments were used for product identification and yield estimations for multi-sulfur products. The OH radicals were generated by

photolysis of O_3 under humid condition using a 253 nm ultraviolet lamp (Philips TUV 16W).

During these experiments, the evolution of 11 sulfur-VOCs was monitored by a Vocus-PTR-LToF-MS, and their oxidation intermediates and products (e.g., sulfur-containing peroxy radicals, gaseous H_2SO_4 and multi-sulfur products) were detected using a nitrate-CI-LToF-MS (Ehn et al., 2014; Krechmer et al., 2018). The Vocus-PTR-LToF-MS detects sulfur-VOCs mainly through proton-transfer reactions between reagent ions (i.e., hydronium ions (H_3O^+) and their water-cluster ions ($(H_2O)_{2\text{-}3}{\cdot}H^+$) and sulfur-VOCs with proton affinities higher than that of water. The nitrate-CI-LToF-MS employs nitrate reagent ions, including NO_3^-, $HNO_3{\cdot}NO_3^-$, and $(HNO_3)_2{\cdot}NO_3^-$, to detect sulfuric acid and highly oxygenated organic oxidation products mainly through nitrate-adduct cluster formation. Additionally, a more detailed description of instrument operation, mass calibration, and calibration procedures is provided in Text S1. The estimation of wall and dilution loss of sulfur-VOCs in our chamber was described in Text S3. The procedure used to quantify sulfur-containing oxygenated organic molecules (sulfur-OOMs) was described in Text S5. In addition, an ozone monitor (Thermo, 49i) and a temperature and humidity sensor (Vaisala HMP110) were used to record O_3 concentration and monitor environmental conditions in the chamber. Due to the chamber is not collapsible, a make-up flow of 15 L/min high-purity zero air generated from zero air generator (AADCO 737 series) was continuously introduced to the chamber and a RH of 20~25% was maintained.

Relative-rate experiments were conducted for selected representative sulfur-VOCs to obtain their •OH reaction rate constants. Isoprene was used as the reference compound because its •OH reaction rate constant at room temperature is well established and k (isoprene + •OH) was taken as 10.00×10^{-11} cm^3 $molecule^{-1}$ s^{-1} at 298 K (Iida et al., 2002; Medeiros et al., 2018). In these experiments, each selected sulfur-VOC was introduced simultaneously with isoprene into the chamber at 298 ± 2 K and 1 atm and their temporal decays were monitored by Vocus-PTR-LToF-MS. The concentrations of sulfur-VOCs and isoprene were corrected for dilution and wall loss before relative-rate analysis. Each relative-rate experiment was conducted in triplicate. Details of the relative-rate calculation, wall/dilution loss correction, and uncertainty estimation are provided in Text S2.

Table 1. Experimental conditions for •OH-initiated oxidation experiments of 11 sulfur-VOCs used for product identification and yield estimations for multi-sulfur products at~~of 11 sulfur-VOCs with •OH under temperature~~ 291±1 K and 1 atm.

Exp.	Species	sulfur-VOCs	Formulae	Molecular structure	Precursor conc. (ppbv)	[O_3] (ppbv)	Relative humidity (%)
1	Monothiols	ethanethiol	C_2H_6S		0.90	33.5	25.1
2					1.50	31.7	24.3
3		1-propanethiol	C_3H_8S		45.39	32.4	17.4
4		2-propanethiol	C_3H_8S		1.10	31.8	24.0
5					1.77	31.5	24.0
6	Dithiols	1,2-ethanedithiol	$C_2H_6S_2$	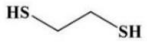	0.65	30.0	23.9
7					1.67	30.5	24.3
8		1,3-propanedithiol	$C_3H_8S_2$		2.84	30.0	22.8
9					2.33	31.1	24.0
10	Acyclic sulfides	dimethyl sulfide	C_2H_6S		0.83	30.9	24.0
11					0.94	31.7	22.0
12		methyl ethyl sulfide	C_3H_8S		0.28	29.5	24.2
13					0.29	31.7	24.3
14		bis(methylthio)methane	$C_3H_8S_2$		10.61	30.4	20.9
15	Cyclic sulfides	trimethylene sulfide	C_3H_6S		0.79	28.6	24.3
16					0.62	29.7	25.3
17		1,3-dithiolane	$C_3H_6S_2$		1.40	35.0	22.8
18					1.23	31.7	24.3
19	Disulfides	dimethyl disulfide	$C_2H_6S_2$	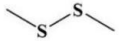	0.74	33.0	25.5
20					0.75	29.0	24.7

2.2 Characteristic of VOC emission from freshwater algae

Fresh water samples with algae were collected from Taihu Lake (approximately ~2338.1 km^2), China, which is the third largest freshwater lake in China(Qin et al., 2019; Wang et al., 2023c), at the Taihu Lake Ecosystem Research Station (Figure S2 a). In the past years, frequent large-scale algal blooms often occurred in Taihu Lake due to anthropogenic nutrient inputs and endogenous pollutant releases in summer(Wang et al., 2019; Xu et al., 2021). Therefore, the water samples with algae taken from Taihu Lake were treated as representative samples of freshwater algae.

During the emission characterization process, water samples were divided into 12 petri dishes (with a total exposed liquid surface area of 0.213 m^2) and placed in the chamber for 18 hours at the temperature of approximately ~21°C to allow the release of VOCs (Figure S2 b). After that, approximately ~90 ppb of O_3 was injected into the chamber and two 253 nm UV lamps were turned on to generate •OH by photolysis of O_3 under humid conditions (Figure S3). A Vocus-PTR-LToF-MS, which was calibrated using selected sulfur-VOC standards (Text S4), was employed to measure and identify sulfur-VOCs and other VOC species released from freshwater algae, as well as their low-oxygenated oxidation products, while a nitrate-CI-LToF-MS was used to identify the mono-sulfur and multi-sulfur products derived from the reactions of sulfur-VOCs from algal source with •OH. A filtration control experiment was also performed to examine whether the detected sulfur-VOCs were associated with algae. The sample was filtered using three stacked layers of ordinary qualitative laboratory filter paper, and the filtration procedure was repeated three times to enhance the removal of visible algal particles. Further details of the filtration control experiment are provided in Text S7.

3 Results and discussion

3.1 Rate constants of sulfur-VOCs with •OH

The •OH reaction rate constants were reported in Table 2 and determined from relative-rate experiments. The selected sulfur-VOCs covered representative functional groups, including monothiol, dithiol, acyclic sulfide, cyclic sulfide, and disulfide. Representative relative-rate plots are shown in Figure 1. The linear relationships between the loss-corrected logarithmic depletion of sulfur-VOCs and that of isoprene indicate that the relative-rate method provides stable constraints on the •OH reaction rate constants under the present experimental conditions. The rate constants obtained in this work span more than one order of magnitude, ranging from $(0.83 \pm 0.08) \times 10^{-11}$ cm^3 $molecule^{-1}$ s^{-1} for DMS to $(26.99 \pm 1.04) \times 10^{-11}$ cm^3 $molecule^{-1}$ s^{-1} for trimethylene sulfide at 298±2 K. ~~The reaction rates were derived based on Eq. (1) in Text S2. By monitoring the change in concentrations of sulfur-VOCs over time, a linear relationship was established. To estimate the •OH concentration in the chamber, DMS was employed as a reference compound, based on its well-~~

established temperature-dependent reaction rate with •OH (Text S2). The estimated •OH concentration was ~4.42 ± 0.08×10^7 molecules cm^{-3}. Using the estimated •OH concentration, the reaction rate constants of 10 other sulfur-VOCs with •OH were subsequently determined (Table 2).

The order of magnitude of reaction rates ranged from 10^{-11} to 10^{-10} cm^3 $molecule^{-1}$ s^{-1} (Table 2), with pronounced differences among different classes of sulfur-VOCs, including thiols, dithiols, acyclic sulfides, cyclic sulfides, and disulfide. Besides the reference compound DMS which was used to estimate •OH concentration in the chamber, Figure 1 presents the linear fitting results for 5 sulfur-VOCs, whose reaction rates remain scarce in previous studies. These 5 sulfur-VOCs and their reaction rates are 1,2-ethanedithiol (2.99 ± 0.10×10^{-10} cm^3 $molecule^{-1}$ s^{-1}), 1,3-propanedithiol (8.46 ± 0.53×10^{-11} cm^3 $molecule^{-1}$ s^{-1}), bis(methylthio)methane (1.49 ± 0.11×10^{-11} cm^3 $molecule^{-1}$ s^{-1}), trimethylene sulfide (1.15 ± 0.02×10^{-10} cm^3 $molecule^{-1}$ s^{-1}), and 1,3-dithiolane (6.11 ± 0.13×10^{-11} cm^3 $molecule^{-1}$ s^{-1}), respectively (Table 2).

The corresponding fittings for the remaining 5 sulfur-VOCs, which have been studied previously, are also provided in Figure S4. The obtained reaction rates of these 4 sulfur-VOCs (i.e., ethanethiol, 1-propanethiol, 2-propanethiol and methyl ethyl sulfide) from our experiments are consistent with that reported by previous studies, ensuring our experimental results (Table 2). However, a notable discrepancy was observed for DMDS, with the current value (1.03 ± 0.02×10^{-10} cm^3 $molecule^{-1}$ s^{-1}) being lower than previously reported ones (1.98 ± 0.18 to 2.39 ± 0.30 ×10^{-10} cm^3 $molecule^{-1}$ s^{-1}), which may be related to the lower temperature in our study and measurement uncertainty due to its rapid rate.

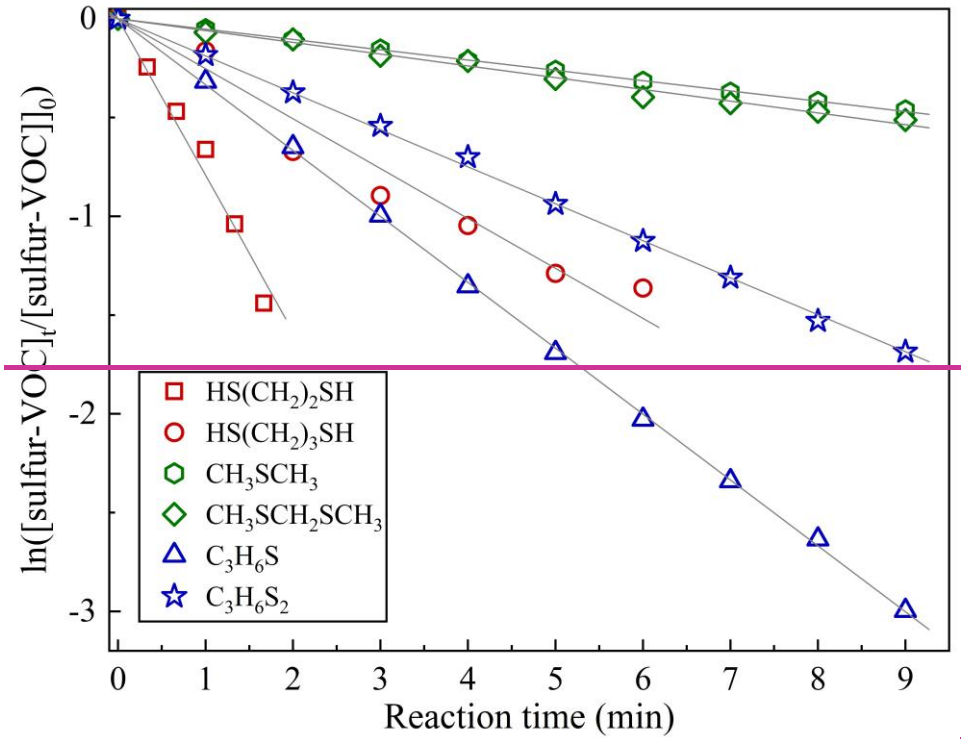

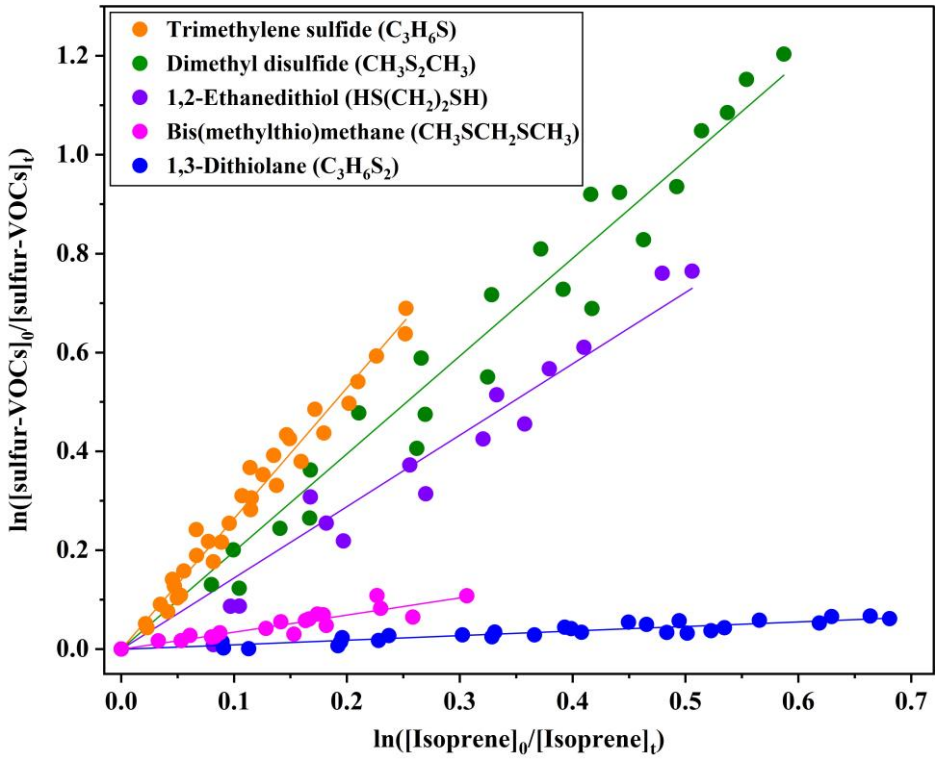

Figure 1. Relative-rate plots for selected sulfur-VOCs using isoprene as the reference compound. The loss-corrected logarithmic depletion of each sulfur-VOC is plotted against that of isoprene. Different colors indicate different sulfur-VOCs, and solid lines denote linear regressions used to derive the •OH reaction rate constants. ~~Plots of $ln([\text{sulfur VOC}]_t/[\text{sulfur VOC}]_0)$ versus reaction time for •OH initiated decay of 1,2-ethanedithiol ($HS(CH)_2SH$), 1,3-propanedithiol ($HS(CH)_3SH$), dimethyl sulfide (CH_3SCH_3), bis(methylthio)methane ($CH_3SCH_2SCH_3$), trimethylene sulfide (C_3H_6S), and 1,3-dithiolane ($C_3H_6S_2$).~~

Table 2. The •OH reaction rate constants of selected sulfur-VOCs determined by the relative-rate method using isoprene as a reference species at 298 ± 2 K~~Inter-comparison of our results with other measurements of reaction rates for 10 sulfur-VOCs with •OH~~.

Species	sulfur-VOCs	Formulae	$k \times 10^{11}$ (cm^3 $molecule^{-1}$ s^{-1})	T (K)	p (Pa)	Buffer gas	Technique [a]	Reference
Monothiol	ethanethiol	CH_3CH_2SH	3.89 ± 0.57	298	1.01×10^5	air	CP-GC	Ref. (Wang et al., 2008)
			4.50 ± 0.50	300	1.01×10^5	N_2	CP-GC	Ref. (Barnes et al., 1986)
			4.21 ± 0.32	298	1.0×10^4	Ar	FP-RF	Ref. (Wine et al., 1984)
			4.44 ± 0.10	291±1	1.01×10^5	air	Vocus-PTR	this work
	1-propanethiol	$CH_3CH_2CH_2SH$	5.30 ± 0.60	300	1.01×10^5	N_2	CP-GC	Ref. (Barnes et al., 1986)
			4.59	298	1.0×10^4	Ar	FP-RF	Ref. (Wine et al., 1984)
			4.51 ± 0.14	291±1	1.01×10^5	air	Vocus-PTR	this work
	2-propanethiol	$(CH_3)_2CHSH$	3.90 ± 0.40	300	1.01×10^5	N_2	CP-GC	Ref. (Barnes et al., 1986)
			4.24	298	1.0×10^4	Ar	FP-RF	Ref. (Wine et al., 1984)
			4.68 ± 0.11	291±1	1.01×10^5	air	Vocus-PTR	this work
Dithiol	1,2-ethanedithiol	$HS(CH_2)_2SH$	29.88 ± 1.02	291±1	1.01×10^5	air	Vocus-PTR	this work
	1,3-propanedithiol	$HS(CH_2)_3SH$	8.46 ± 0.53	291±1	1.01×10^5	air	Vocus-PTR	this work
Acyclic sulfide	methyl ethyl sulfide	$CH_3SCH_2CH_3$	1.50 ± 0.29	297	1.01×10^5	air	GC-FID	Ref. (Wang et al., 2011)
			1.16 ± 0.42	298	1.01×10^5	air	RK-FTIR	Ref. (Oksdath-Mansilla et al.,
			1.46 ± 0.36	298	1.01×10^5	air	CP-GC	Ref. (Wang et al., 2008)
			1.54 ± 0.04	291±1	1.01×10^5	air	Vocus-PTR	this work
	bis(methylthio)methane	$CH_3SCH_2SCH_3$	1.49 ± 0.11	291±1	1.01×10^5	air	Vocus-PTR	this work
Cyclic sulfide	trimethylene sulfide	C_3H_6S	11.53 ± 0.21	291±1	1.01×10^5	air	Vocus-PTR	this work
	1,3-dithiolane	$C_3H_6S_2$	6.11 ± 0.13	291±1	1.01×10^5	air	Vocus-PTR	this work
Disulfide	dimethyl disulfide	$CH_3S_2CH_3$	23.90 ± 3.00	297	1466	N_2	HPF-LIF	Ref. (Abbatt et al., 1992)
			19.80 ± 1.80	298	6666-26664	Ar	FP-RF	Ref. (Wine et al., 1981)
			22.30 ± 8.00	298	1.01×10^5	air	CP-GC	Ref. (Cox and Sheppard, 1980)
			10.26 ± 0.20	291±1	1.01×10^5	air	Vocus-PTR	this work

Species	sulfur-VOCs	Formulae	$k \times 10^{11}$ (cm^3 $molecule^{-1}$ s^{-1})	T (K)	p (Pa)	Buffer gas	Technique[a]	Reference
Monothiol	ethanethiol	CH_3CH_2SH	3.89 ± 0.57	298	1.01×10^5	air	CP-GC	(Wang et al., 2008)
			4.50 ± 0.50	300	1.01×10^5	N_2	CP-GC	(Barnes et al., 1986)
			4.21 ± 0.32	298	1.0×10^4	Ar	FP-RF	(Wine et al., 1984)
			4.51 ± 0.32	298±2	1.01×10^5	air	Vocus-PTR	This work
Dithiol	1,2-ethanedithiol	$HS(CH_2)_2SH$	14.36 ± 0.26	298±2	1.01×10^5	air	Vocus-PTR	This work
Acyclic sulfide	dimethyl sulfide	CH_3SCH_3	0.87 ± 0.03	298	1.01×10^5	air	CP-GC	(Wang et al., 2008)
			0.78 ± 0.18	299	1.01×10^5	air	CP-FTIR	(Albu et al., 2005)
			0.80 ± 0.05	298±3	1.01×10^5	air	CP-GC	(Barnes et al., 1988)
			0.83 ± 0.08	298±2	1.01×10^5	air	Vocus-PTR	This work
	bis(methylthio)methane	$CH_3SCH_2SCH_3$	3.50 ± 0.09	298±2	1.01×10^5	air	Vocus-PTR	This work
Cyclic sulfide	trimethylene sulfide	C_3H_6S	26.99 ± 1.04	298±2	1.01×10^5	air	Vocus-PTR	This work
	1,3-dithiolane	$C_3H_6S_2$	0.95 ± 0.05	298±2	1.01×10^5	air	Vocus-PTR	This work
Disulfide	dimethyl disulfide	$CH_3S_2CH_3$	23.90 ± 3.00	297	1466	N_2	HPF-LIF	(Abbatt et al., 1992)
			19.80 ± 1.80	298	6666-26664	Ar	FP-RF	(Wine et al., 1981)
			22.30 ± 8.00	298	1.01×10^5	air	CP-GC	(Cox and Sheppard, 1980)
			20.18 ± 1.53	298±2	1.01×10^5	air	Vocus-PTR	This work

Note: The rate constants reported in this work were obtained from additional relative-rate experiments using isoprene as the reference compound. The •OH reaction rate constant of isoprene was taken as 10.00×10^{-11} cm^3 $molecule^{-1}$ s^{-1} at 298 K (Iida et al., 2002; Medeiros et al., 2018). The uncertainties of this work represent the standard deviations of triplicate measurements.

[a] CP: continuous photolysis; GC: gas chromatography; FTIR: Fourier transform infrared spectroscopy; FP: flash photolysis; RF: resonance fluorescence; HPF: high-pressure fast flow; LIF: laser-induced fluorescence

[a] CP: Continuous Photolysis. GC: Gas Chromatography. FP: Flash Photolysis. RF: Resonance Fluorescence. FID: Flame Ionization Detection. RK: Rapid Kinetic. FTIR: Fourier Transform Infrared Spectroscopy. HPF: High Pressure Fast. LIF: Laser Induced FluorescenceFor species with available literature data, the relative-rate-derived values agree well with previous values. For ethanethiol, the rate constant obtained in this work is (4.51 ± 0.32) × 10^{-11} cm^3 $molecule^{-1}$ s^{-1}, which is consistent with previously reported values of (3.89 ± 0.57) to (4.50 ± 0.50) × 10^{-11} cm^3 $molecule^{-1}$ s^{-1} near room temperature (Barnes et al., 1986; Wang et al., 2008; Wine et al., 1984). For DMS, the rate constant obtained in this work is (0.83 ± 0.08) × 10^{-11} cm^3 $molecule^{-1}$ s^{-1}, also consistent with that from previous studies. For DMDS ($CH_3S_2CH_3$), the relative-rate-derived value obtained in this work is (20.18 ± 1.53) × 10^{-11} cm^3 $molecule^{-1}$ s^{-1}, which agrees well with previously reported values of (19.80 ± 1.80) to (23.90 ± 3.00) × 10^{-11} cm^3 $molecule^{-1}$ s^{-1} at 297-298 K (Abbatt et al., 1992; Cox and Sheppard, 1980; Wine et al., 1981). These agreements supports the reliability of our relative-rate method and the obtained kinetic dataset.

The relative-rate results further show that •OH reactivity depends strongly on molecular structures of sulfur-VOCs, but not in a simple monotonic way with either sulfur atom number or cyclic structure. The dithiol 1,2-ethanedithiol ($HS(CH_2)_2SH$) exhibits a relatively high-rate constant of (14.36 ± 0.26) × 10^{-11} cm^3 $molecule^{-1}$ s^{-1}, consistent with the high reactivity of S-H functional groups toward •OH. For thiols, previous kinetic and theoretical studies have shown that H-abstraction from the S-H group is an important and efficient initiation reaction pathway with •OH, leading to the formation of sulfur-centered radicals (Atkinson and Arey, 2003; Cruz-Torres and Galano, 2007; Douroudgari et al., 2020; Mai et al., 2020). The presence of S-H groups therefore provides reactive H-abstraction sites and can enhance overall •OH reactivity, which is also consistent with previous experimental rate-constant measurements for aliphatic thiols (Barnes et al., 1986; Wang et al., 2008; Wine et al., 1984). However, the comparison among sulfur-VOCs also indicates that the number of sulfur atoms alone does not determine the rate constants. For example, bis(methylthio)methane ($CH_3SCH_2SCH_3$) contains two sulfur atoms but shows a moderate rate constant of (3.50 ± 0.09) × 10^{-11} cm^3 $molecule^{-1}$ s^{-1}, behaving kinetically more like an acyclic sulfide than a highly reactive dithiol or disulfide.

The two cyclic sulfides investigated show contrasting reactivities. Trimethylene sulfide (C_3H_6S) exhibits the highest rate constant ((26.99 ± 1.04) × 10^{-11} cm^3 $molecule^{-1}$ s^{-1}) among the selected sulfur-VOCs. This high reactivity is likely associated with its strained three-membered ring structure, which may facilitate •OH-initiated reaction pathways. In contrast, 1,3-dithiolane ($C_3H_6S_2$) shows a lower rate constant of (0.95 ± 0.05) × 10^{-11} cm^3 $molecule^{-1}$ s^{-1}. This contrast indicates that cyclic structure alone does not necessarily lead to enhanced •OH reactivity, and ring strain, sulfur functionality, and specific molecular configuration need to be considered together.

Acyclic and cyclic sulfides can react with •OH through both H-abstraction from α-C-H bonds and •OH-addition to the sulfur atom. Previous studies have shown that the •OH-addition pathway can become more competitive under lower-temperature conditions (Barnes et al., 2006; Ye et al., 2022). Because the rate constants reported here are derived from overall precursor decay, the observed values represent the combined contribution of possible initiation pathways, and the relative branching between H-abstraction and •OH-addition cannot be directly separated in the present experiments. Overall, the kinetic results demonstrate that the •OH reaction rate constants of sulfur-VOCs depend on molecular features, such as reactive S-H groups, sulfur functionality, α-C-H sites and ring strain. ~~Based on these measured rate constants, molecular structure-reactivity relationships can be observed among the investigated sulfur-VOCs, as illustrated in Figure 2. Sulfur-VOCs containing S-H functional groups, such as thiols and dithiols, generally react more rapidly with •OH than acyclic sulfides, reflecting the high reactivity of the S-H bond toward H-abstraction by •OH. For dithiols, the presence of two S-H groups provides multiple accessible H-abstraction sites for •OH and thus can enhance the overall reactivity. The higher rate observed for 1,2-ethanedithiol ($HS(CH_2)_2SH$) relative to 1,3-propanedithiol ($HS(CH_2)_3SH$) may further hint the importance of vicinal configuration of the two S-H groups.~~

~~Acyclic sulfides, which lack S-H functional groups, typically exhibit lower reaction rates because their oxidation by •OH proceeds mainly through abstraction from α-C-H bonds, which are less reactive than S-H bonds. Notably, disulfides react faster than acyclic sulfides despite also lacking S-H groups, highlighting the activating role of the S-S bond in facilitating radical formation during the initial •OH attack. Bis(methylthio)methane ($CH_3SCH_2SCH_3$), although containing two sulfur atoms, behaves kinetically more like an acyclic sulfide, indicating that the presence of an S-S bond is a key structural factor enhancing reactivity.~~

~~Cyclic sulfides display intermediate reactivity, with reaction rates that are higher than those of acyclic sulfides. This behavior is likely influenced by ring strain, owing to stronger ring strain, such as that in trimethylene sulfide (C_3H_6S), can enhance reactivity by lowering the barrier for H-abstraction. Overall, the reaction rates of sulfur-VOCs with •OH increase when molecules containing more reactive S-H, S-S bond and cyclic structure, whereas compounds are limited primarily to H-abstraction from α-C-H bonds generally react more slowly.~~

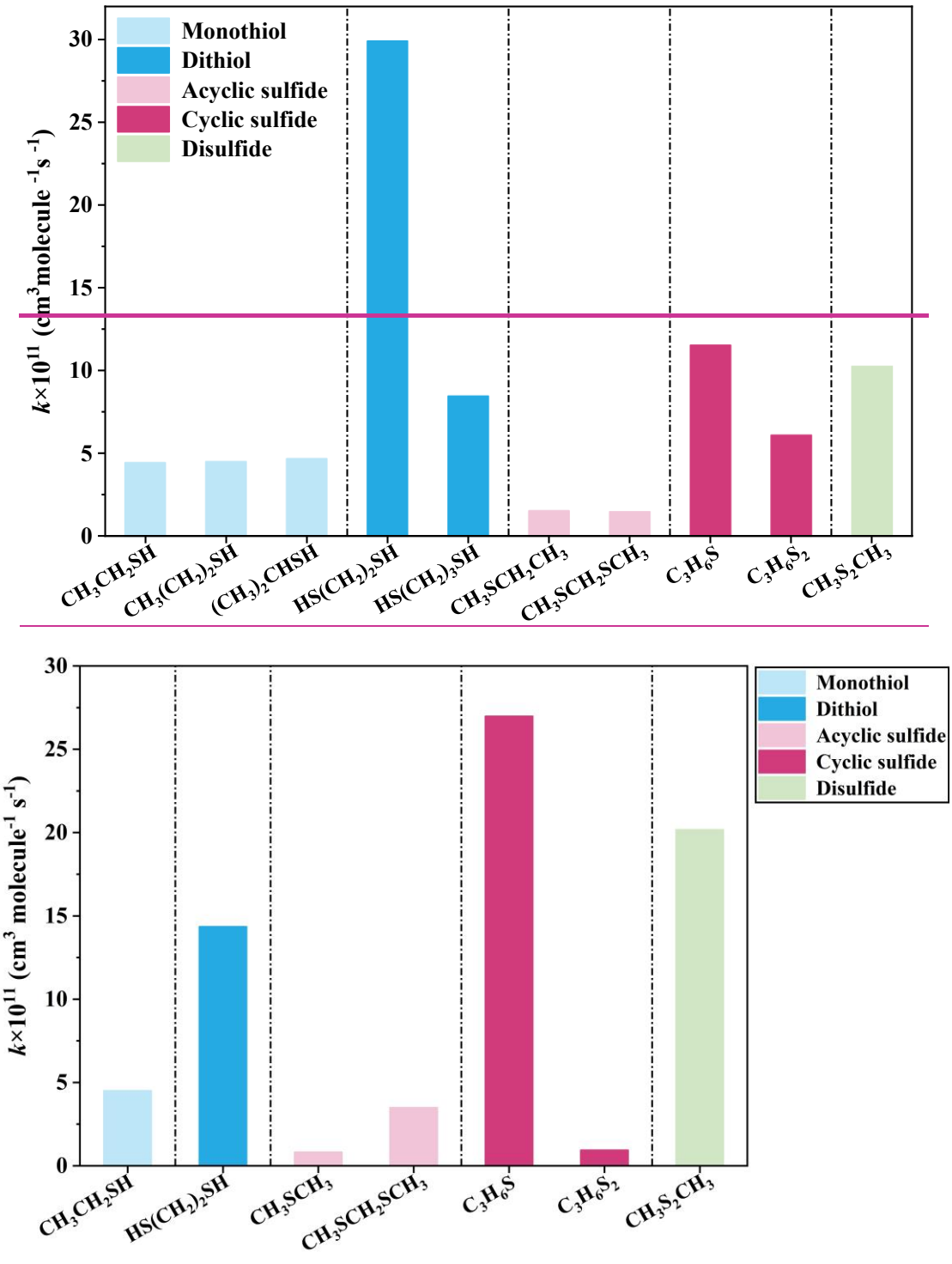

Figure 2. Reaction rates of 7~~10~~ sulfur-VOCs with •OH, divided by their functional groups.

3.2 Formation of multi-sulfur products

During our chamber experiments, many multi-sulfur products which contain 2 sulfur atoms in their chemical formulas were detected by nitrate-CI-LToF-MS (Table S3). The formation pathways of multi-sulfur products from •OH-initiated oxidation of 11 selected sulfur-VOCs under NO_x-free conditions were investigated. The 11 sulfur-VOCs examined here comprise 5 thiols (CH_3CH_2SH,

$CH_3(CH_2)_2SH$, $(CH_3)_2CHSH$, $HS(CH_2)_2SH$, $HS(CH_2)_3SH$), 3 acyclic sulfides (CH_3SCH_3, $CH_3CH_2SCH_3$, $CH_3SCH_2SCH_3$), 2 cyclic sulfides (C_3H_6S, $C_3H_6S_2$) and 1 disulfide ($CH_3S_2CH_3$). Among them, to exhibit the formation pathways of multi-sulfur products, DMS and $HS(CH_2)_3SH$ are adopted as representative compounds for acyclic sulfides and thiols, respectively, whereas DMDS is treated as a representative compound for disulfide.

The reactions between DMS and •OH primarily proceed via two competing pathways (Scheme 1). One is that •OH adds to sulfur atom to form $CH_3S•(OH)CH_3$. Another is that •OH abstracts H-atom from the methyl group to generate the $CH_3SCH_2•$. These primary radicals subsequently react with O_2 to form a series of sulfur-containing $RO_2•$, including the initially formed DMS-derived $RO_2•$ (e.g., $CH_3SCH_2OO•$), as well as other sulfur-containing $RO_2•$ intermediates (Berndt et al., 2023; Goss and Kroll, 2023; Shen et al., 2022). Notably, under NO_x-free conditions, sulfur-containing $RO_2•$ are not efficiently removed by NO, and their subsequent fate is expected to involve competition among unimolecular isomerization via H-migration, and bimolecular reactions of $RO_2•$ + $HO_2•$ and $RO_2•$ + $R'O_2•$ (Jenkin et al., 2003; Orlando and Tyndall, 2012). Recent studies of DMS oxidation have shown that H-shift isomerization of $CH_3SCH_2OO•$ can be an important pathway associated with hydroperoxymethyl thioformate (HPMTF) formation (Berndt et al., 2019; Jernigan et al., 2022; Ye et al., 2022). In the box-model analysis of DMS oxidation by •OH, this H-shift process was included to evaluate its competition with bimolecular reactions of $RO_2•$ (Text S6; Figure. S7). The model results indicate that H-shift dominates the initial fate of $CH_3SCH_2OO•$ under the present chamber conditions. However, based~~(i.e., $CH_3SOO•$, $CH_3S(O)OO•$, and $CH_3S(O)_3OO•$). Notably, under NO_x-free conditions, these sulfur-containing $RO_2•$ tend to undergo bimolecular reactions with another $R'O_2•$ and $HO_2•$, instead of termination by NO_x. Under NO_x-free conditions, the fate of sulfur-$RO_2•$ is primarily determined by the competition between $RO_2•$ + $HO_2•$ and $RO_2•$ + $R'O_2•$ reactions. Box-model simulation shows that $RO_2•$ + $R'O_2•$ reactions initially dominate the reaction system, but their relative contribution gradually decreases to approximately 50% as the reaction proceeds (Text S6; Figure S7 and S8). This sustained and substantial participation of $RO_2•$ + $R'O_2•$ underscores its critical role in generating the observed multi-sulfur products. Based~~ on the detection by nitrate-CI-LToF-MS, various multi-sulfur bimolecular products (e.g., $C_2H_6O_4S_2$ and $C_2H_6O_5S_2$) resulting from $RO_2•$-$R'O_2•$ reactions were still identified (Figure ~~S6~~S5). Among these, $C_2H_6O_4S_2$ may originate from the bimolecular reaction of $CH_3SOO•$ with $CH_3S(O)_2OO•$ or the self-polymerization of $CH_3S(O)OO•$, while $C_2H_6O_5S_2$ may be formed by the bimolecular reaction between $CH_3S(O)_2OO•$ and $CH_3S(O)OO•$ (Scheme 1).

~~Previous~~ Although previous studies on the •OH-initiated oxidation of DMS have extensively investigated the formation and fate of sulfur-$RO_2•$, and have highlighted the potential importance of $RO_2•$-$R'O_2•$ reactions, particularly under low-NO_x or NO_x-free conditions (Barnes et al., 2006; Ye

et al., 2022). However, direct molecular-level identification of multi-sulfur products has been very limited in earlier studies. Most previous investigations mainly focused on major oxidation products such as C_2H_6OS (dimethyl sulfoxide), $C_2H_6O_2S$ (dimethyl sulfone), CH_4SO_3, and SO_2, rather than explicit characterization of individual bimolecular products from RO_2•-$R'O_2$• chemistry (Chen et al., 2023; Hatakeyama et al., 1982). Self- and cross-reactions of RO_2• are known to produce organic peroxides (ROOR') and multimeric products, and such pathways have been experimentally confirmed for a variety of alkyl peroxy radicals (Cho et al., 2023; Nozière, 2025; Orlando and Tyndall, 2012). In addition, studies on highly oxygenated organic molecules (HOMs) formation from biogenic VOC oxidation have demonstrated that RO_2•-$R'O_2$• reactions can lead to complex, multifunctional products that are efficiently detected using nitrate-CIMS (Bianchi et al., 2019; Ehn et al., 2014; Gao et al., 2023). Nevertheless, there have been no previous reports explicitly identifying molecular formulas such as $C_2H_6O_4S_2$ and $C_2H_6O_5S_2$ as products of RO_2•-$R'O_2$• reactions in the atmospheric oxidation of sulfur-VOCs. The formation of these multi-sulfur products can likely be favored by low-NO_x and NO_x-free experimental conditions, which can prolong the lifetime of sulfur-containing RO_2• and favor their bimolecular reactions.

As shown in Scheme S1, the •OH-initiated oxidation of DMDS follows a reaction framework similar to that of sulfides. Cleavage of the S-S bond leads to the formation of sulfur-centered radical intermediates which are analogous to those generated from acyclic sulfides. Among the multi-sulfur products detected from the •OH-initiated oxidation of DMDS, $C_2H_6O_4S_2$ was identified under the present experimental conditions, and its formation is also derived from RO_2•-$R'O_2$• bimolecular reactions inferred for the DMS oxidation system.

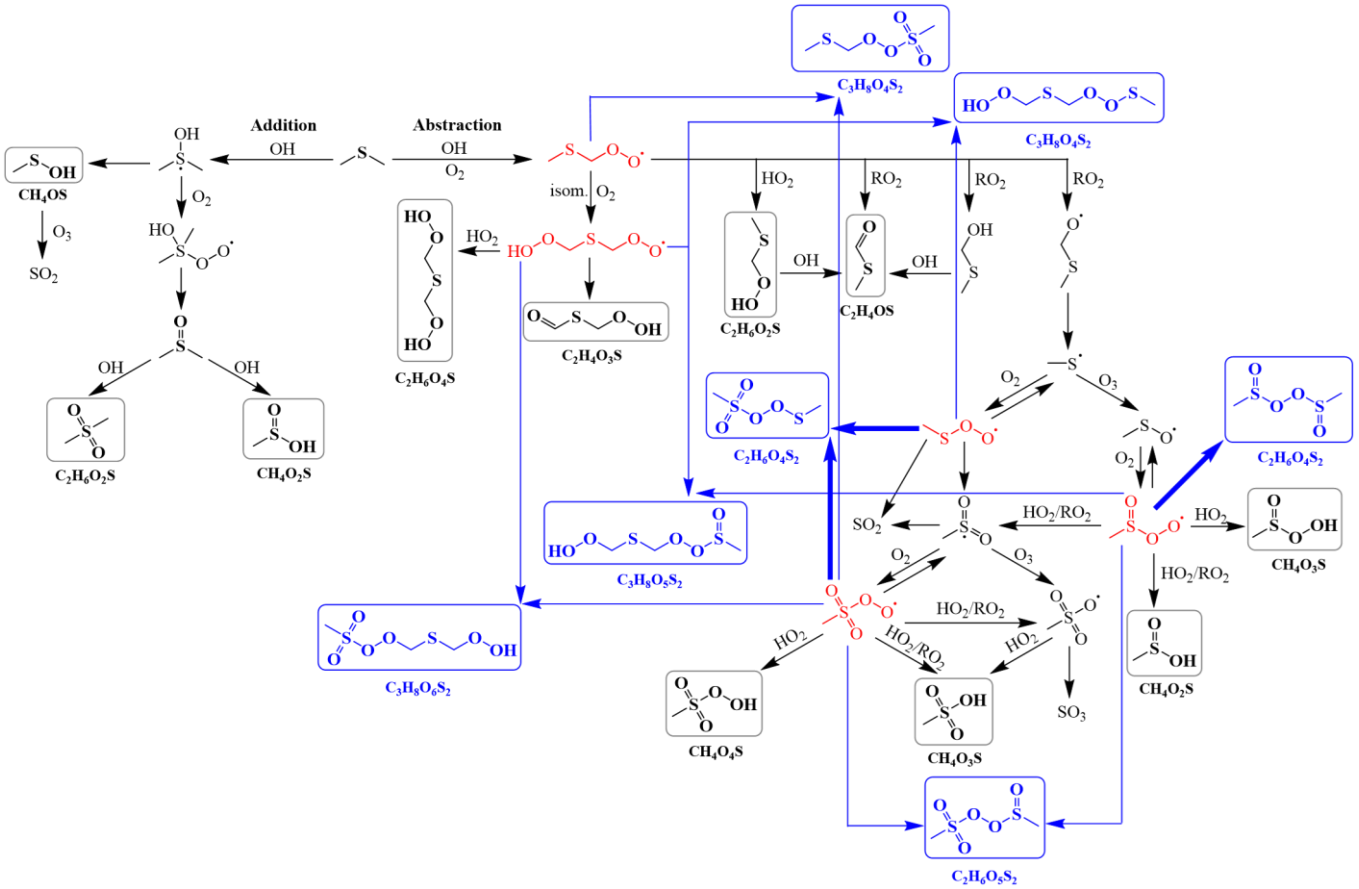

Scheme 1. Scheme of the reaction pathways of DMS (CH_3SCH_3) with •OH. Gray boxes denote mono-sulfur oxygenated organic products detected by Vocus-PTR-LToF-MS and nitrate-CI-LToF-MS. Blue boxes indicate multi-sulfur products detected by nitrate-CI-LToF-MS and these multi-sulfur products are presumably generated by the red-labeled sulfur-containing RO_2 radicals via bimolecular reactions. The bold blue arrows highlight the potential dominant pathways leading to the abundant multi-sulfur products.

For thiols, the reactions between $HS(CH_2)_3SH$ and •OH are initiated predominantly by H-abstraction from the S-H group (Scheme 2), forming the sulfur-centered radical ($HS(CH_2)_3S$•) (Berndt et al., 2023; Douroudgari et al., 2020; Mai et al., 2020). Subsequent reactions lead to the formation of a few sulfur-containing RO_2• intermediates, including $HS(CH_2)_3OO$•, $HOO(CH_2)_3SOO$•, and $HOO(CH_2)_3S(O)_2OO$•. Compared to RO_2• derived from acyclic sulfides and disulfides, thiol-derived RO_2• exhibit more structurally diverse, enabling more bimolecular reaction pathways. As a result, more multi-sulfur products were identified (Figure S10), including $C_6H_{14}O_8S_2$, $C_6H_{14}O_9S_2$, $C_6H_{14}O_{10}S_2$, etc. Plausible formation pathways for these multi-sulfur products are illustrated in Scheme 2. Specifically, $C_6H_{14}O_9S_2$ can originate from the bimolecular reaction of $HOO(CH_2)_3S(O)_2OO$• with $HOO(CH_2)_3S(O)OO$•. The formation pathways of $C_6H_{14}O_8S_2$ and $C_6H_{14}O_{10}S_2$ are similar with $C_6H_{14}O_9S_2$. In addition, multi-sulfur products were also detected for other investigated sulfur-VOCs (Figures ~~S9~~ S8 and ~~S11~~S10-~~S13~~S12). Although acyclic sulfides and disulfides are structurally distinct, the reaction pathways presented above indicates that their •OH-initiated oxidation proceeds through similar sulfur-centered radical intermediates and subsequent reactions of sulfur-RO_2•.

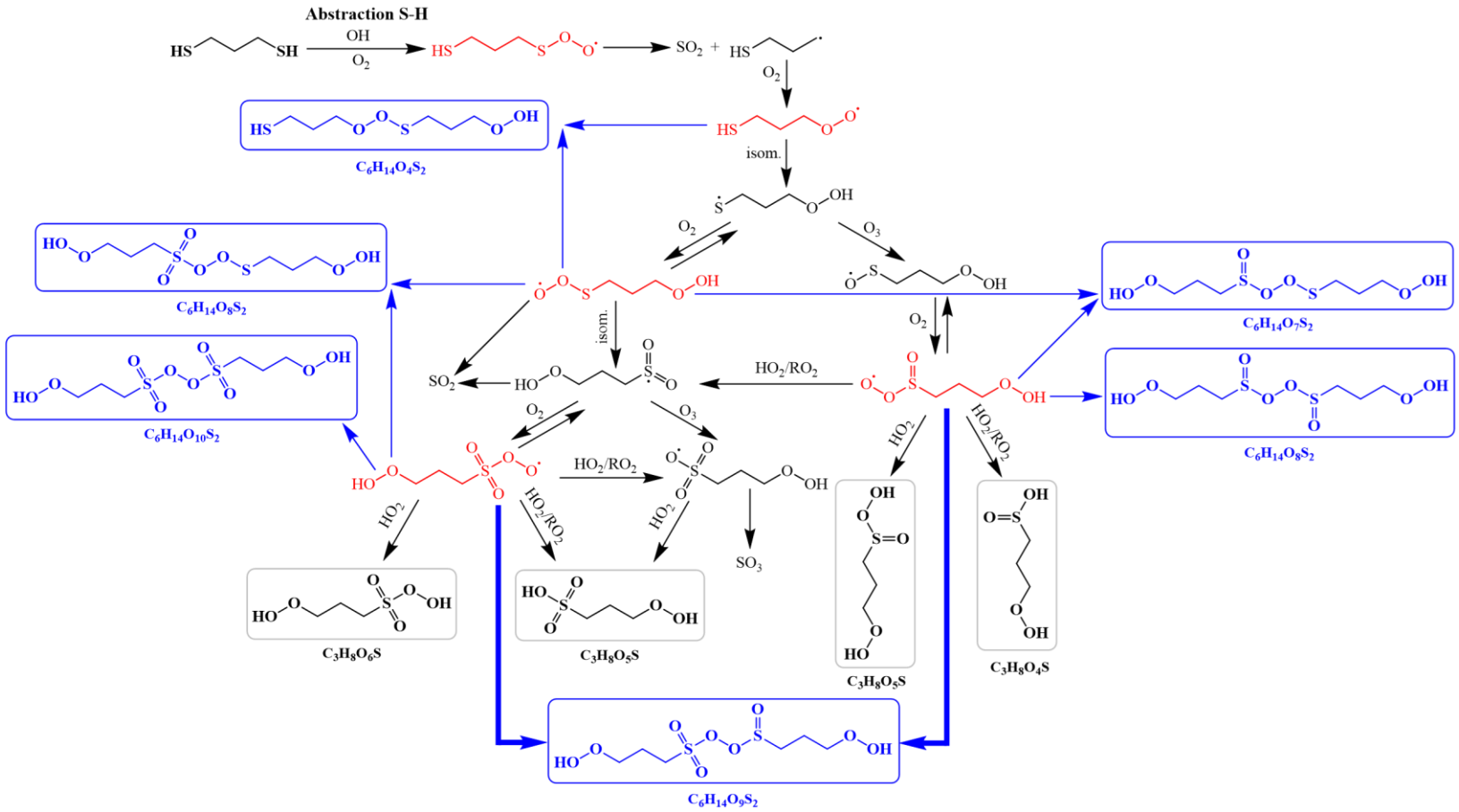

Scheme 2. Scheme of the reaction pathways of $HS(CH_2)_3SH$ with •OH. Gray boxes denote mono-sulfur oxygenated organic products detected by Vocus-PTR-LToF-MS and nitrate-CI-LToF-MS. Blue boxes indicate multi-sulfur products detected by nitrate-CI-LToF-MS and these multi-sulfur products are presumably generated by the red-labeled sulfur-containing RO_2 radicals via bimolecular reactions. The bold blue arrows highlight the potential dominant pathways leading to the abundant multi-sulfur products

To evaluate the yields and volatility distributions of these multi-sulfur products, Figure 3 summarizes the estimated volatility distributions and formation yields from the •OH-initiated oxidation of 10 sulfur-VOCs except for ethanethiol. No multi-sulfur products were detected for ethanethiol, suggesting that their formation was either negligible or that the resulting concentrations were below the detection limit of the nitrate-CI-LToF-MS. The volatilities were estimated using the parameterization proposed by (Li et al., 2016). Overall, the total yields of multi-sulfur products varied substantially among the 10 sulfur-VOCs, ranging from 0.001% to 11.73% (Table S3), indicating a strong dependence on precursor structure and sulfur functionality.

Among all investigated compounds, trimethylene sulfide (C_3H_6S) exhibited the highest total yield (11.73%), suggesting its highly efficient formation of multi-sulfur products. In contrast, several thiol systems and certain acyclic sulfides produced only trace amounts of multi-sulfur products, with total yields below 0.1%. Acyclic sulfides and disulfide systems (e.g., DMS) predominantly generated semi-volatile organic compounds (SVOCs), with total multi-sulfur yields generally below ~4%. In comparison, cyclic sulfides displayed more diverse volatility distributions. For C_3H_6S, multi-sulfur products extended into the low-volatility organic compounds (LVOCs) and extremely low-volatility organic compounds (ELVOCs) regimes, with a significant fraction of the total yield residing in these low-volatility classes. By contrast, 1,3-dithiolane ($C_3H_6S_2$) mainly produced SVOCs-range multi-sulfur products, and individual species yields remained below ~0.4%, despite a moderate summed yield. Thiols (e.g., $HS(CH_2)_3SH$) exhibited a distinct pattern: although their oxidation generated products extending into the LVOCs and ELVOCs regimes, the overall formation efficiency was low, with total yields ranging from 0.001% to 0.40%. This suggests that structural factors, such as the position and number of -SH groups, may influence both RO_2• reactivity and multi-sulfur product formation efficiency. The presence of LVOCs and ELVOCs multi-sulfur products, particularly for cyclic sulfides, implies a potential role in secondary organic aerosol formation and particle growth.

It should be noted that the semi-quantification of these multi-sulfur products is based on the calibration factor of gaseous sulfuric acid (H_2SO_4) (Text S2) , a common approach in nitrate-CIMS measurements due to the lack of authentic standards for highly oxygenated organic compounds (Ehn et al., 2014; Jokinen et al., 2012).. It was assumed that the ionization efficiency of H_2SO_4 towards the reagent ions ($(HNO_3)_nNO_3^-$, n=0, 1 and 2) is the same as that of multi-sulfur products. As a result, the reported yields may have an additional uncertainty because of ionization efficiency difference between H_2SO_4 and multi-sulfur products towards the reagent ions , as discussed in previous studies (Ehn et al., 2014; Hyttinen et al., 2015).

. Although the formation yields of many detected multi-sulfur products are relatively low, their low volatility indicates SOA forming potential. The reported yields represent only the gas-phase multi-sulfur products detected by nitrate-CI-LToF-MS and should not be interpreted as total

oxidation product yields. A substantial fraction of sulfur may be converted to inorganic sulfur products and mono-sulfur oxidation products, such as SO_2, H_2SO_4, sulfoxides, sulfones, methanesulfonic acid, and other mono-sulfur oxygenated compounds, which are not included in the reported multi-sulfur product yields. In addition, nitrate-CI-LToF-MS preferentially detects highly oxygenated and low-volatility compounds, while more volatile or less oxygenated sulfur-containing products may be underrepresented. Product wall loss and possible particle-phase transfer may further reduce the observed gas-phase concentrations of multi-sulfur products. Therefore, the reported yields should be treated as lower-limit gas-phase yields of multi-sulfur products.

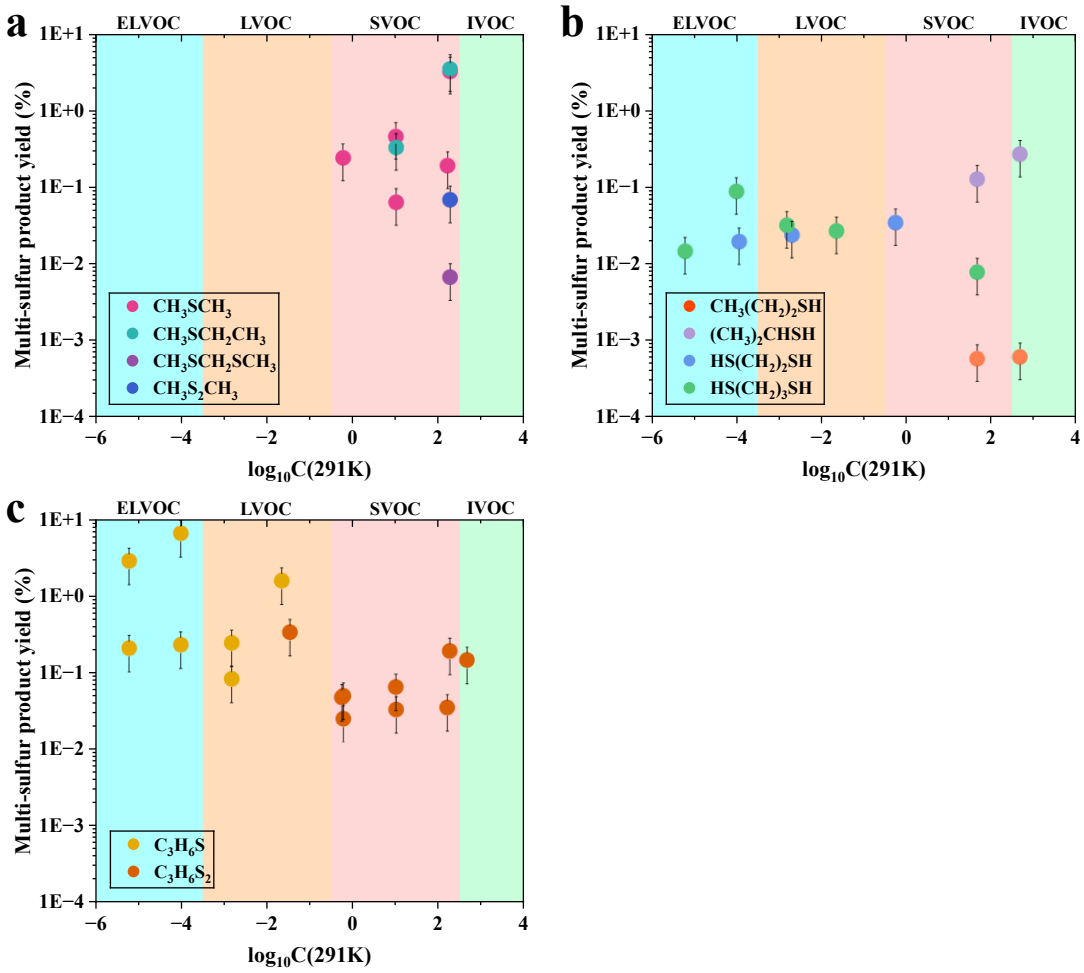

Figure 3. Volatility ($log_{10}C^*$, at 291 K) versus the yield (%) of multi-sulfur products formed from the •OH-initiated oxidation of sulfur-VOCs. (a) acyclic sulfides and disulfide: CH_3SCH_3, $CH_3SCH_2CH_3$, $CH_3SCH_2SCH_3$ and $CH_3S_2CH_3$; (b) thiols: $CH_3(CH_2)_2SH$, $(CH_3)_2CHSH$, $HS(CH_2)_2SH$, and $HS(CH_2)_3SH$; (c) cyclic sulfides: C_3H_6S, $C_3H_6S_2$. The volatility ranges were divided into ELVOCs, LVOCs, SVOCs and IVOCs (intermediate volatile organic compounds). Error bars represent an estimated uncertainty of approximately ±50%, primarily arising from the use of calibration factor of gaseous H_2SO_4.

3.3 Identification and atmospheric oxidation of sulfur-VOCs and other VOCs emitted from freshwater algae

As shown in Figure 4a, the emitted VOCs from freshwater algae were measured by Vocus-PTR-LToF-MS and 240 compounds in total were identified, including 143 CHO species, 43 CH species, 20 sulfur-VOCs, and 34 other VOCs. High-resolution peak fittings for the assigned sulfur-VOCs were shown in Figure S15. The molecular formulas and mixing ratios of 20 sulfur-VOCs are summarized in Table ~~S4~~ S5 and Figure 4b.

Under the specific treatment conditions (see Section 2.2), ~~absolute~~ mixing ratios of emitted VOCs spanned over three orders of magnitude, ranging from 0.01 to 11.77 ppbv. Among the 20 identified sulfur-VOCs, 6 monosulfur species were detected and they are dominated ones. Specifically, CH_4S

reached the highest level (11.77 ppbv), followed by C_2H_6S (8.60 ppbv), CH_2S (4.09 ppbv), and C_2H_4S (3.57 ppbv), while the remaining monosulfur species were present at sub-ppbv levels. 9 disulfur species were identified with generally lower abundances, spanning from 0.04 to 0.78 ppbv, with $C_6H_{14}S_2$ (0.78 ppbv) and $C_3H_6S_2$ (0.69 ppbv) representing the most abundant disulfur species. 3 trisulfur species were detected at similarly low levels, ranging from 0.06 to 0.50 ppbv, with $C_4H_{10}S_3$ showing the highest mixing ratio within this group. In contrast, 2 tetrasulfur species were the least abundant, with mixing ratios decreasing to ~0.01 ppbv for $C_2H_6S_4$ and $C_3H_6S_4$. Overall, a clear and systematic decrease in mixing ratios was observed with increasing sulfur number. Because Vocus-PTR-LToF-MS measurements constrain molecular formulas rather than isomer-specific structures, isomeric species (e.g., DMS and ethanethiol, C_2H_6S) cannot be distinguished solely by their exact mass and may have different sensitivities. Therefore, the reported mixing ratios should be interpreted as semi-quantitative apparent ones rather than definitive isomer-specific concentrations.

In addition, photographs taken before and after repeated filtrations show that the green algal suspension became nearly clear, indicating effective removal of most visible algal biomass (Figure S16). Consistently, removal of algal biomass by repeated filtrations through stacked qualitative filter papers led to a remarkable decrease in the abundance of sulfur-VOCs (Figure S17), suggesting that the emissions of sulfur-VOCs were closely associated with the algal biological processes. ~~removal of most algae by filtration led to a remarkable decrease in sulfur-VOC signals (Figure S16), supporting that these sulfur-VOCs were primarily associated with freshwater algae.~~ Although only molecular formulas rather than structures could be assigned, the results still provide a comprehensive inventory of freshwater algae-emitted sulfur-VOCs. However, because the freshwater lake samples contained natural microbial communities and the filtration procedure was not designed to sterilize the samples or fully remove bacteria, this experiment cannot distinguish direct algal emissions or other biological processing. Notably, the molecular formulas of sulfur-VOCs targeted in our chamber study were also present in the list of sulfur-VOCs emitted from freshwater algae. Although Vocus-PTR-LToF-MS measurements constrain molecular formulas rather than isomer-specific structures, the co-occurrence of these formula families in algal emissions supports the atmospheric relevance of the structure-resolved kinetics and oxidation mechanisms derived from our chamber experiments.

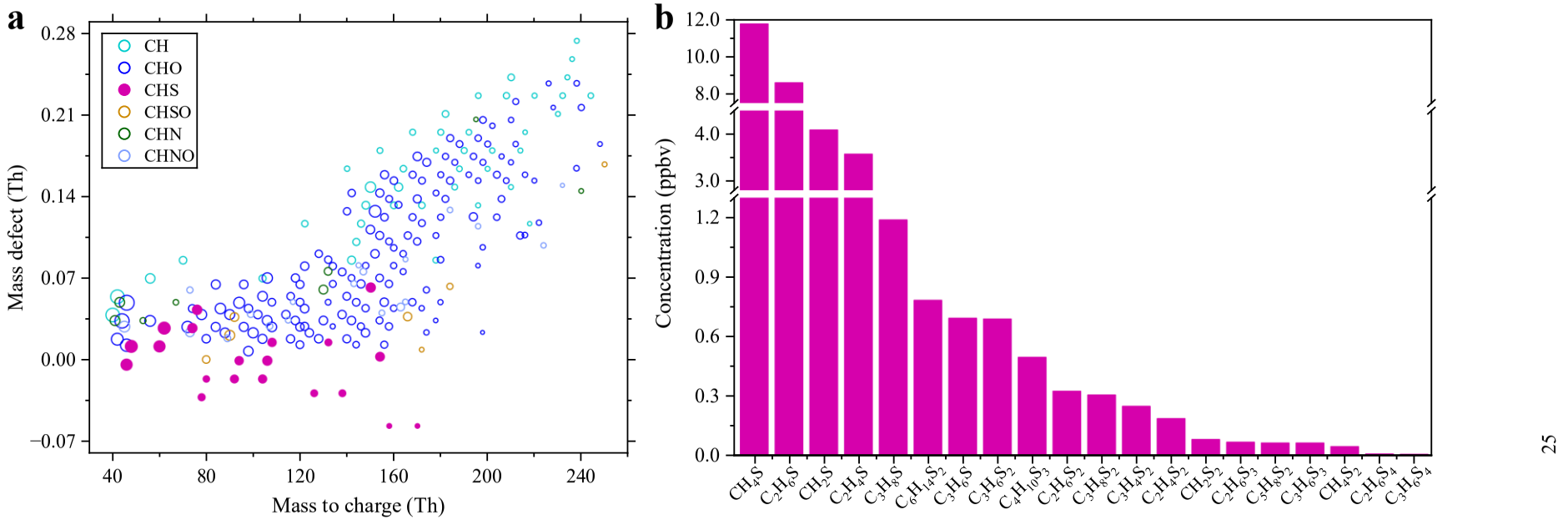
a
CH
CHO
CHS
CHSO
CHN
CHNO
Mass defect (Th)
Mass to charge (Th)
b
Concentration (ppbv)
CH_4S
C_2H_6S
CH_2S
C_2H_4S
C_3H_8S
$C_6H_{14}S_2$
C_3H_6S
$C_3H_6S_2$
$C_4H_{10}S_3$
$C_2H_6S_2$
$C_3H_8S_2$
$C_3H_4S_2$
$C_2H_4S_2$
CH_2S_2
$C_2H_6S_3$
$C_3H_8S_2$
$C_3H_6S_3$
CH_4S_2
$C_2H_6S_4$
$C_3H_6S_4$

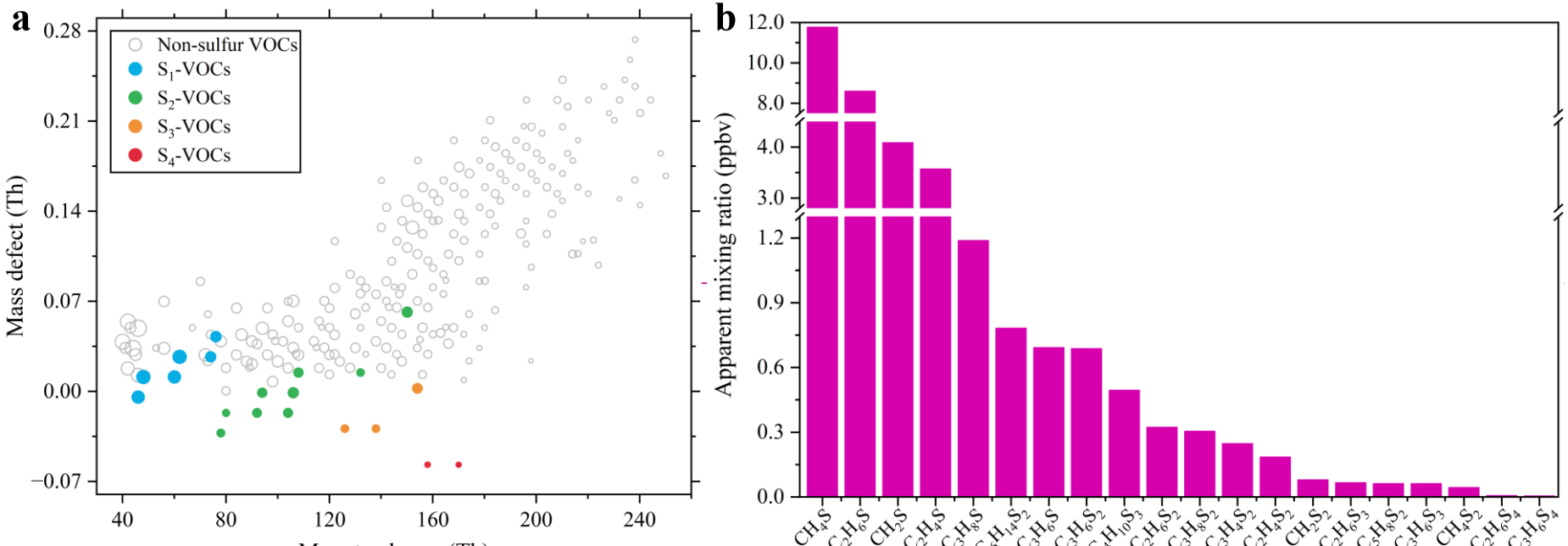
a
Non-sulfur VOCs
S_1-VOCs
S_2-VOCs
S_3-VOCs
S_4-VOCs
Mass defect (Th)
b
Apparent mixing ratio (ppbv)
CH_4S
C_2H_6S
CH_2S
C_2H_4S
C_3H_8S
$C_6H_{14}S_2$
C_3H_6S
$C_3H_6S_2$
$C_4H_{10}S_3$
$C_2H_6S_2$
$C_3H_8S_2$
$C_3H_4S_2$
$C_2H_4S_2$
CH_2S_2
$C_2H_6S_3$
$C_3H_8S_2$
$C_3H_6S_3$
CH_4S_2
$C_2H_6S_4$
$C_3H_6S_4$

Figure 4. (a) Mass-defect plot of VOCs detected by Vocus-PTR-LToF-MS before oxidation. The 20 sulfur-VOCs are highlighted and grouped according to the number of sulfur atoms in their assigned molecular formulas, while non-sulfur VOCs are shown in gray. Marker size represents normalized PTR-MS signal intensity rather than calibrated concentration. (b) Semi-quantitative mixing ratios of the 20 sulfur-VOCs detected from the algal emissions.~~(a) Mass-defect plot of emitted VOCs from freshwater algae measured by Vocus PTR-LToF-MS, with data points color-coded by elemental composition (CH, CHO, CHS, CHSO, CHN, and CHNO) and marker size scaled to signal intensity. (b) Mixing ratios of the 20 sulfur-VOCs detected from the algal emissions~~

In subsequent atmospheric oxidation experiments of these emitted VOCs including sulfur-VOCs, our chamber was maintained under NO_x-free conditions, hence the termination of RO_2• by NO_x was suppressed and bimolecular reactions of RO_2• were favored. Approximately 110 oxidation products were identified using nitrate-CI-LToF-MS, including dozens of mono-sulfur organic compounds, a few inorganic sulfur-containing species (e.g., H_2SO_4 and its clusters), and 11 multi-sulfur products (Figure 5 and Table S5). Among 11 multi-sulfur products, 7 of them could be inferred from our selected sulfur-VOCs chamber simulation experiments and their high-resolution peak fitting plots were also shown in Figure ~~S17~~S18. Additionally, 4 multi-sulfur products could not be reproduced from our chamber simulation experiments (Figure ~~S18~~S19). These experimental results not only provide evidence that multi-sulfur products can be formed from bimolecular reactions of sulfur-containing RO2• under low-NOx conditions, but also improve our understanding of the atmospheric oxidation chemistry of algae-emitted sulfur-VOCs in ambient air (especially in low NO_x environments). Notably, the detection of H_2SO_4 and its clusters, which are well-established precursors for atmospheric new particle formation, suggests that the oxidation of algae-emitted sulfur-VOCs may contribute to secondary particle formation (Jokinen et al., 2012; Lee et al., 2019; Yao et al., 2018). These findings expand the current understanding of the atmospheric processing of biogenic sulfur-VOCs released from freshwater algae and suggest that their chemical complexity may have broader implications for sulfur transformation and secondary aerosol formation.~~These experimental results not only confirm that multi-sulfur products can be formed from bimolecular reactions of sulfur-RO_2•, but also promote the understanding of atmospheric chemical processes of sulfur-VOCs in ambient air (especially in low NO_x environments). Notably, the detection of H_2SO_4 and its clusters known as precursors for new particle formation suggests that the oxidation of algae-emitted sulfur-VOCs can contribute to secondary particle formation.~~ However, due to the complex composition of algae-derived sulfur-VOCs, specific formation pathways of these multi-sulfur products need to be further elucidated.

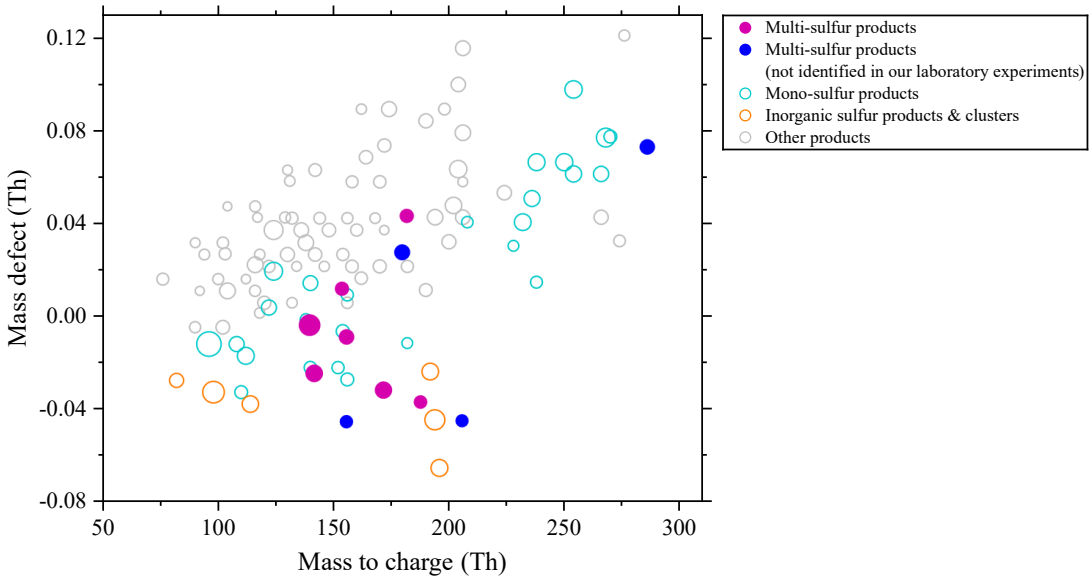

Figure 5. Mass defect plot of oxidation products detected by nitrate-CI-LToF-MS during~~formed from~~ the •OH-initiated oxidation of algae-emitted VOCs. Multi-sulfur products shown in deep purple represent species whose molecular formulas were also identified in our chamber simulation experiments of the selected sulfur-VOCs, whereas those shown in dark blue represent multi-sulfur products whose corresponding molecular formulas were not identified in our chamber experiments. Marker size is proportional to the corresponding signal intensity.

Although the oxidation experiments were conducted under NO_x-free conditions, such chemical regimes are still representative of atmospherically relevant environments characterized by low NO_x levels and strong biogenic sulfur-VOC emissions (e.g., inland eutrophic lakes, remote marine boundary layer and polar regions). In these environments, NO_x concentrations are typically very low and RO_2• termination by NO_x is strongly suppressed, while RO_2• + HO_2• and RO_2• + $R'O_2$• pathways may become more important (Berresheim et al., 1998; Novak et al., 2022; Read et al., 2008; Steinke et al., 2018). Field observations in these environments have reported sulfur-VOCs such as DMS and methanthiol at dozens to hundreds of pptv levels (Berresheim et al., 1998; Novak et al., 2022; Read et al., 2008). Therefore, multi-sulfur products derived from RO_2•-$R'O_2$• bimolecular reactions during atmospheric oxidation of sulfur-VOCs may have SOA forming potential~~ contribute SOA formation~~ in these environments. While the quantitative contribution of sulfur-VOCs-derived multi-sulfur products to SOA formation remains uncertain, the present results only highlight the detection and formation pathways of multi-sulfur products from atmospheric oxidation of sulfur-VOCs.

4 Conclusions

This study provides an integrated understanding of kinetics and formation pathways of multi-

sulfur products of •OH-initiated oxidation of a series of selected sulfur-VOCs with different functional groups. The kinetic results show that •OH reactivity is strongly influenced by molecular structure, including reactive S-H groups, sulfur functionality, α-C-H sites, molecular configuration, and ring strain. Under low-NO_x chamber conditions,~~Reaction rate constants determined for these sulfur-VOCs reveal clear structure–reactivity relationships and~~ sulfur-RO_2• can undergo bimolecular reactions under low NOx, leading to the formation of multi-sulfur products with distinct volatility characteristics. Acyclic sulfides and disulfides mainly produce semi-volatile multi-sulfur products with relatively higher yields, whereas thiols (particularly dithiols) favor the formation of more highly oxygenated, low-volatility products that may promote SOA formation. Furthermore, the selected sulfur-VOCs were also observed from the emission of freshwater algae and some of multi-sulfur products derived from our chamber simulation experiments of selected sulfur-VOCs were also identified from •OH-initiated oxidation of VOCs emitted from freshwater algae. These results together further confirm the atmospheric relevance of these selected sulfur-VOCs and the sulfur-RO_2• chemistry leading to the formation of multi-sulfur products.

Biogenic sulfur-VOCs could have increased significance in the context of ongoing changes in the atmospheric sulfur budget. Anthropogenic SO_2 emissions have been declining worldwide, reducing the dominance of the traditional gaseous H_2SO_4 formation pathway from anthropogenic SO_2 in atmospheric sulfur cycling (Crippa et al., 2016; Smith et al., 2011; Zheng et al., 2018). In addition to anthropogenic SO_2, natural sulfur sources such as H_2S, DMS-derived SO_2, and naturally emitted SO_2, including passive volcanic SO_2 emissions, can also contribute to gaseous H_2SO_4 and particulate sulfate formation (Bates et al., 1992; Faloona, 2009; Yvon and Saltzman, 1996). In this evolving context, the relative contribution of biogenic sulfur-VOCs become increasingly important, particularly in low-NO_x environments. Our results demonstrate that, in addition to conventional oxidation pathways, sulfur-containing RO_2• bimolecular reactions can lead to the formation of low-volatility multi-sulfur products, providing an additional pathway linking sulfur-VOCs to secondary aerosol formation.~~Instead, the oxidation of biogenic sulfur-VOCs is likely to become an increasingly important source for gaseous H_2SO_4 and particulate sulfate, particularly in low-NO_x environments. The formation of low-volatility multi-sulfur products via sulfur-RO_2• bimolecular reactions highlight an additional pathway by which sulfur-VOCs can contribute to SOA formation.~~ Overall, this study underscores the growing role of biogenic sulfur-VOCs in atmospheric sulfur budget and highlights the necessity of explicitly considering the atmospheric chemistry of sulfur-VOCs in atmospheric models.

Data availability. The data used to support the conclusions in this study are available at a public data repository of Zenodo via https://doi.org/10.5281/zenodo.18923240. Additional data related to

this paper can be requested from the authors (lei_yao@fudan.edu.cn).

Author contributions. L.Y. conceived and designed this study and revised the manuscript. X.R. conducted the experiments, performed data analysis, and prepared the manuscript with contributions from all co-authors. C.L. assisted in designing the experiments. C.A. and G.Y. assisted with data collection. J.L.S, R.L.C., D. R. Worsnop, and L.W. interpreted the results and revised the manuscript.

Competing interests. The contact author has declared that none of the authors has any competing interests.

Acknowledgements. This research was supported by the National Natural Science Foundation of China (22376031) and the National Key Research and Development Program of China (2022YFC3704100) ~~and the National Natural Science Foundation of China (22376031)~~.

References

Abbatt, J. P. D., Fenter, F. F., and Anderson, J. G.: High-pressure discharge flow kinetics study of hydroxyl + dimethyl sulfide, dimethyl disulfide .fwdarw. products from 297 to 368 K, J. Phys. Chem., 96, 1780–1785, https://doi.org/10.1021/j100183a053, 1992.

Albu, M., Barnes, I., Becker, K. H., Patroescu-Klotz, I., Mocanu, R., and Benter, T.: Rate coefficients for the gas-phase reaction of OH radicals with dimethyl sulfide: temperature and O 2 partial pressure dependence, Phys. Chem. Chem. Phys., 8, 728–736, https://doi.org/10.1039/b512536g, 2005.

Andreae, M. O. and Raemdonck, H.: Dimethyl Sulfide in the Surface Ocean and the Marine Atmosphere: A Global View, Science, 221, 744–747, https://doi.org/10.1126/science.221.4612.744, 1983.

Atkinson, R. and Arey, J.: Atmospheric Degradation of Volatile Organic Compounds, Chem. Rev., 103, 4605–4638, https://doi.org/10.1021/cr0206420, 2003.

Atkinson, R., Baulch, D. L., Cox, R. A., Crowley, J. N., Hampson, R. F., Hynes, R. G., Jenkin, M. E., Rossi, M. J., and Troe, J.: Evaluated kinetic and photochemical data for atmospheric chemistry: Volume I - gas phase reactions of O_x, HO_x, NO_x and SO_x species, Atmos. Chem. Phys., 4, 1461–1738, https://doi.org/10.5194/acp-4-1461-2004, 2004.

Bao, Q., Wu, A., Lu, J., Jiang, L., and Shen, Q.: Analysis of Three Dimethyl Sulfides in Freshwater Lakes Using Headspace Solid-Phase Microextraction-Gas Chromatography with Flame Photometric Detection, Atmosphere, 15, 484, https://doi.org/10.3390/atmos15040484, 2024.

Barnes, I., Bastian, V., Becker, K. H., Fink, E. H., and Nelsen, W.: Oxidation of sulphur compounds in the atmosphere: I. Rate constants of OH radical reactions with sulphur dioxide, hydrogen sulphide, aliphatic thiols and thiophenol, J. Atmos. Chem., 4, 445–466, https://doi.org/10.1007/bf00053845, 1986.

Barnes, I., Bastian, V., and Becker, K. H.: Kinetics and mechanisms of the reaction of OH radicals with dimethyl sulfide, Int. J. Chem. Kinet., 20, 415–431, https://doi.org/10.1002/kin.550200602, 1988.

Barnes, I., Hjorth, J., and Mihalopoulos, N.: Dimethyl Sulfide and Dimethyl Sulfoxide and Their Oxidation in the Atmosphere, Chem. Rev., 106, 940–975, https://doi.org/10.1021/cr020529+, 2006.

Bates, T. S., Lamb, B. K., Guenther, A., Dignon, J., and Stoiber, R. E.: Sulfur emissions to the atmosphere from natural sourees, J. Atmos. Chem., 14, 315–337, https://doi.org/10.1007/bf00115242, 1992.

Berndt, T., Scholz, W., Mentler, B., Fischer, L., Hoffmann, E. H., Tilgner, A., Hyttinen, N., Prisle, N. L., Hansel, A., and Herrmann, H.: Fast Peroxy Radical Isomerization and OH Recycling in the

Reaction of OH Radicals with Dimethyl Sulfide, J. Phys. Chem. Lett., 10, 6478–6483, https://doi.org/10.1021/acs.jpclett.9b02567, 2019.

Berndt, T., Hoffmann, E. H., Tilgner, A., Stratmann, F., and Herrmann, H.: Direct sulfuric acid formation from the gas-phase oxidation of reduced-sulfur compounds, Nat. Commun., 14, 4849, https://doi.org/10.1038/s41467-023-40586-2, 2023.

Berndt, T., Hoffmann, E. H., Tilgner, A., and Herrmann, H.: Gas-Phase Formation of Sulfurous Acid (H2SO3) in the Atmosphere, Angew. Chem. Int. Ed., e202405572, https://doi.org/10.1002/anie.202405572, 2024.

Berresheim, H., Huey, J. W., Thorn, R. P., Eisele, F. L., Tanner, D. J., and Jefferson, A.: Measurements of dimethyl sulfide, dimethyl sulfoxide, dimethyl sulfone, and aerosol ions at Palmer Station, Antarctica, J. Geophys. Res.: Atmos., 103, 1629–1637, https://doi.org/10.1029/97jd00695, 1998.

Bianchi, F., Kurtén, T., Riva, M., Mohr, C., Rissanen, M. P., Roldin, P., Berndt, T., Crounse, J. D., Wennberg, P. O., Mentel, T. F., Wildt, J., Junninen, H., Jokinen, T., Kulmala, M., Worsnop, D. R., Thornton, J. A., Donahue, N., Kjaergaard, H. G., and Ehn, M.: Highly Oxygenated Organic Molecules (HOM) from Gas-Phase Autoxidation Involving Peroxy Radicals: A Key Contributor to Atmospheric Aerosol, Chem. Rev., 119, 3472–3509, https://doi.org/10.1021/acs.chemrev.8b00395, 2019.

Charlson, R. J., Lovelock, J. E., Andreae, M. O., and Warren, S. G.: Oceanic phytoplankton, atmospheric sulphur, cloud albedo and climate, Nature, 326, 655–661, https://doi.org/10.1038/326655a0, 1987.

Chen, J., Lane, J. R., and Kjaergaard, H. G.: Reaction of Atmospherically Relevant Sulfur-Centered Radicals with RO2 and HO2, J. Phys. Chem. A, 127, 2986–2991, https://doi.org/10.1021/acs.jpca.3c00558, 2023.

Cho, J., Mulvihill, C. R., Klippenstein, S. J., and Sivaramakrishnan, R.: Bimolecular Peroxy Radical (RO2) Reactions and Their Relevance in Radical Initiated Oxidation of Hydrocarbons, J. Phys. Chem. A, 127, 300–315, https://doi.org/10.1021/acs.jpca.2c06960, 2023.

Cox, R. A. and Sheppard, D.: Reactions of OH radicals with gaseous sulphur compounds, Nature, 284, 330–331, https://doi.org/10.1038/284330a0, 1980.

Crippa, M., Janssens-Maenhout, G., Dentener, F., Guizzardi, D., Sindelarova, K., Muntean, M., Dingenen, R. V., and Granier, C.: Forty years of improvements in European air quality: regional policy-industry interactions with global impacts, Atmos. Chem. Phys., 16, 3825–3841, https://doi.org/10.5194/acp-16-3825-2016, 2016.

Cruz-Torres, A. and Galano, A.: On the Mechanism of Gas-Phase Reaction of C1−C3 Aliphatic Thiols + OH Radicals, J. Phys. Chem. A, 111, 1523–1529, https://doi.org/10.1021/jp0673415, 2007.

Dai, Y., Yang, S., Zhao, D., Hu, C., Xu, W., Anderson, D. M., Li, Y., Song, X.-P., Boyce, D. G., Gibson, L., Zheng, C., and Feng, L.: Coastal phytoplankton blooms expand and intensify in the 21st century, Nature, 615, 280–284, https://doi.org/10.1038/s41586-023-05760-y, 2023.

Deng, K., Huo, J., Wang, Y., Wang, L., Yin, S., Li, C., Li, Y., Yang, G., Yao, L., Fu, Q., and Wang, L.: Characteristics of atmospheric reduced-sulfur compounds at a suburban site of Shanghai, J. Environ. Sci., 156, 671–683, https://doi.org/10.1016/j.jes.2024.06.030, 2025.

Douroudgari, H., Vahedpour, M., and Mohammadi, S.: Atmospheric reaction of methyl mercaptan with hydroxyl radical as an acid rain primary agent, Sci. Rep., 10, 18081, https://doi.org/10.1038/s41598-020-74767-6, 2020.

Du, L., Xu, Y., Ge, M., and Jia, L.: Rate constant for the reaction of ozone with diethyl sulfide, Atmos. Environ., 41, 7434–7439, https://doi.org/10.1016/j.atmosenv.2007.05.041, 2007.

Ehn, M., Thornton, J. A., Kleist, E., Sipilä, M., Junninen, H., Pullinen, I., Springer, M., Rubach, F., Tillmann, R., Lee, B., Lopez-Hilfiker, F., Andres, S., Acir, I.-H., Rissanen, M., Jokinen, T., Schobesberger, S., Kangasluoma, J., Kontkanen, J., Nieminen, T., Kurtén, T., Nielsen, L. B., Jørgensen, S., Kjaergaard, H. G., Canagaratna, M., Maso, M. D., Berndt, T., Petäjä, T., Wahner, A., Kerminen, V.-M., Kulmala, M., Worsnop, D. R., Wildt, J., and Mentel, T. F.: A large source of low-volatility secondary organic aerosol, Nature, 506, 476–479, https://doi.org/10.1038/nature13032, 2014.

Faloona, I.: Sulfur processing in the marine atmospheric boundary layer: A review and critical assessment of modeling uncertainties, Atmos. Environ., 43, 2841–2854, https://doi.org/10.1016/j.atmosenv.2009.02.043, 2009.

Fiddes, S. L., Woodhouse, M. T., Utembe, S., Schofield, R., Alexander, S. P., Alroe, J., Chambers, S. D., Chen, Z., Cravigan, L., Dunne, E., Humphries, R. S., Johnson, G., Keywood, M. D., Lane, T. P., Miljevic, B., Omori, Y., Protat, A., Ristovski, Z., Selleck, P., Swan, H. B., Tanimoto, H., Ward, J. P., and Williams, A. G.: The contribution of coral-reef-derived dimethyl sulfide to aerosol burden over the Great Barrier Reef: a modelling study, Atmos. Chem. Phys., 22, 2419–2445, https://doi.org/10.5194/acp-22-2419-2022, 2021.

Gao, Y., Lu, K., and Zhang, Y.: Review of technologies and their applications for the speciated detection of RO2 radicals, J. Environ. Sci., 123, 487–499, https://doi.org/10.1016/j.jes.2022.09.028, 2023.

Goss, M. B. and Kroll, J. H.: Chamber studies of OH + dimethyl sulfoxide and dimethyl disulfide: insights into the dimethyl sulfide oxidation mechanism, Atmos. Chem. Phys., 24, 1299–1314, https://doi.org/10.5194/acp-24-1299-2024, 2023.

Hashemi, S. R., Saheb, V., and Hosseini, S. M. A.: Theoretical kinetic study of the reaction between dimethyl disulfide and OH radicals, J. Sulfur Chem., 40, 185–194, https://doi.org/10.1080/17415993.2018.1556274, 2019.

Hatakeyama, S., Okuda, M., and Akimoto, H.: Formation of sulfur dioxide and methanesulfonic acid in the photooxidation of dimethyl sulfide in the air, Geophys. Res. Lett., 9, 583–586, https://doi.org/10.1029/gl009i005p00583, 1982.

Huang, H., Xu, X., Liu, X., Han, R., Liu, J., and Wang, G.: Distributions of four taste and odor compounds in the sediment and overlying water at different ecology environment in Taihu Lake, Sci. Rep., 8, 6179, https://doi.org/10.1038/s41598-018-24564-z, 2018.

Iida, Y., Obi, K., and Imamura, T.: Rate Constant for the Reaction of OH Radicals with Isoprene at 298±2 K, Chem. Lett., 31, 792–793, https://doi.org/10.1246/cl.2002.792, 2002.

Jenkin, M. E., Saunders, S. M., Wagner, V., and Pilling, M. J.: Protocol for the development of the Master Chemical Mechanism, MCM v3 (Part B): tropospheric degradation of aromatic volatile organic compounds, Atmos. Chem. Phys., 3, 181–193, https://doi.org/10.5194/acp-3-181-2003, 2003.

Jernigan, C. M., Fite, C. H., Vereecken, L., Berkelhammer, M. B., Rollins, A. W., Rickly, P. S., Novelli, A., Taraborrelli, D., Holmes, C. D., and Bertram, T. H.: Efficient Production of Carbonyl Sulfide in the Low-NOx Oxidation of Dimethyl Sulfide, Geophys. Res. Lett., 49, https://doi.org/10.1029/2021gl096838, 2022.

Jokinen, T., Lehtipalo, K., Thakur, R. C., Ylivinkka, I., Neitola, K., Sarnela, N., Laitinen, T., Kulmala, M., Petäjä, T., and Sipilä, M.: Measurement report: Long-term measurements of aerosol precursor concentrations in the Finnish subarctic boreal forest, Atmos. Chem. Phys., 22, 2237–2254, https://doi.org/10.5194/acp-22-2237-2022, 2022.

Kiene, R. and Service, S.: Decomposition of dissolved DMSP and DMS in estuanne waters: dependence on temperature and substrate concentration, Mar. Ecol. Prog. Ser., 76, 1–11, https://doi.org/10.3354/meps076001, 1991.

Kiene, R. P.: Production of methanethiol from dimethylsulfoniopropionate in marine surface waters, Mar. Chem., 54, 69–83, https://doi.org/10.1016/0304-4203(96)00006-0, 1996.

Kiene, R. P. and Taylor, B. F.: Demethylation of Dimethylsulfoniopropionate and Production of Thiols in Anoxic Marine Sediments, Appl. Environ. Microbiol., 54, 2208–2212, https://doi.org/10.1128/aem.54.9.2208-2212.1988, 1988.

Kiene, R. P., Linn, L. J., and Bruton, J. A.: New and important roles for DMSP in marine microbial communities, J. Sea Res., 43, 209–224, https://doi.org/10.1016/s1385-1101(00)00023-x, 2000.

Kietäväinen, R., Nyyssönen, M., Nuppunen-Puputti, M., and Bomberg, M.: Naturally occurring volatile organic compounds in deep bedrock groundwater, Commun. Earth Environ., 6, 64, https://doi.org/10.1038/s43247-025-02053-2, 2025.

Kilgour, D. B., Novak, G. A., Sauer, J. S., Moore, A. N., Dinasquet, J., Amiri, S., Franklin, E. B., Mayer, K., Winter, M., Morris, C. K., Price, T., Malfatti, F., Crocker, D. R., Lee, C., Cappa, C. D., Goldstein, A. H., Prather, K. A., and Bertram, T. H.: Marine gas-phase sulfur emissions during an induced phytoplankton bloom, Atmos. Chem. Phys., 22, 1601–1613, https://doi.org/10.5194/acp-22-1601-2022, 2021.

Krechmer, J., Lopez-Hilfiker, F., Koss, A., Hutterli, M., Stoermer, C., Deming, B., Kimmel, J., Warneke, C., Holzinger, R., Jayne, J., Worsnop, D., Fuhrer, K., Gonin, M., and Gouw, J. de: Evaluation of a New Reagent-Ion Source and Focusing Ion–Molecule Reactor for Use in Proton-Transfer-Reaction Mass Spectrometry, Anal. Chem., 90, 12011–12018, https://doi.org/10.1021/acs.analchem.8b02641, 2018.

Li, C., Yao, L., Wang, Y., Fang, M., Chen, X., Wang, L., Li, Y., Yang, G., and Wang, L.: Formation of chlorinated organic compounds from Cl atom-initiated reactions of aromatics and their detection in suburban Shanghai, Atmos. Chem. Phys., 25, 11247–11260, https://doi.org/10.5194/acp-25-11247-2025, 2025.

Li, Y., Pöschl, U., and Shiraiwa, M.: Molecular corridors and parameterizations of volatility in the chemical evolution of organic aerosols, Atmos. Chem. Phys., 16, 3327–3344, https://doi.org/10.5194/acp-16-3327-2016, 2016.

Li, Y., Gong, X., Zhao, Z., Shen, Q., and Zhang, L.: Distribution and Release of Volatile Organic Sulfur Compounds in Yangcheng Lake, Water, 14, 1199, https://doi.org/10.3390/w14081199, 2022.

Lily, M., Hynniewta, S., Lv, X., Chandra, A. K., Tchinda, N. T., and Du, L.: Assessing the Isomerization of a Primary Intermediate (CH 3 SCH 2 O 2 • Radical) in Dimethyl Sulfide Degradation in the Marine Boundary Layer, ACS Earth Space Chem., 7, 2129–2138, https://doi.org/10.1021/acsearthspacechem.3c00209, 2023.

Liu, M., Wu, T., Zhao, X., Zan, F., Yang, G., and Miao, Y.: Cyanobacteria blooms potentially enhance volatile organic compound (VOC) emissions from a eutrophic lake: Field and experimental evidence, Environ. Res., 202, 111664, https://doi.org/10.1016/j.envres.2021.111664, 2021.

Lu, X., Fan, C., Shang, J., Deng, J., and Yin, H.: Headspace solid-phase microextraction for the determination of volatile sulfur compounds in odorous hyper-eutrophic freshwater lakes using gas chromatography with flame photometric detection, Microchem. J., 104, 26–32, https://doi.org/10.1016/j.microc.2012.04.001, 2012.

Mai, T. V.-T., Nguyen, H. T., and Huynh, L. K.: Kinetics of hydrogen abstraction from CH3SH by OH radicals: An ab initio RRKM-based master equation study, Atmos. Environ., 242, 117833, https://doi.org/10.1016/j.atmosenv.2020.117833, 2020.

Medeiros, D. J., Blitz, M. A., James, L., Speak, T. H., and Seakins, P. W.: Kinetics of the Reaction of OH with Isoprene over a Wide Range of Temperature and Pressure Including Direct Observation of Equilibrium with the OH Adducts, J. Phys. Chem. A, 122, 7239–7255, https://doi.org/10.1021/acs.jpca.8b04829, 2018.

Mynard, C., Franklin, E. B., Alroe, J., Somerville, N., Patti, A., Siems, S. T., Williams, A., Mallet, M. D., Humphries, R., and Dunne, E.: Constraining Atmospheric Methanethiol Estimates Over the Southern Ocean, Geophys. Res. Lett., 52, https://doi.org/10.1029/2025gl116470, 2025.

Novak, G. A., Kilgour, D. B., Jernigan, C. M., Vermeuel, M. P., and Bertram, T. H.: Oceanic emissions of dimethyl sulfide and methanethiol and their contribution to sulfur dioxide production in the marine atmosphere, Atmos. Chem. Phys., 22, 6309–6325, https://doi.org/10.5194/acp-22-6309-2022, 2022.

Nozière, B.: Trends in organic peroxide (ROOR) formation in the reactions of C1–C4 alkyl peroxy radicals (RO 2) in gas, Chem. Sci., 16, 16590–16596, https://doi.org/10.1039/d5sc03559g, 2025.

Oksdath-Mansilla, G., Peñéñory, A. B., Albu, M., Barnes, I., Wiesen, P., and Teruel, M. A.: CH3CH2SCH3 + OH radicals: temperature-dependent rate coefficient and product identification under atmospheric pressure of air, J. Phys. Org. Chem., 23, 925–930, https://doi.org/10.1002/poc.1714, 2010.

Orlando, J. J. and Tyndall, G. S.: Laboratory studies of organic peroxy radical chemistry: an overview with emphasis on recent issues of atmospheric significance, Chem. Soc. Rev., 41, 6294, https://doi.org/10.1039/c2cs35166h, 2012.

Qin, B., Paerl, H. W., Brookes, J. D., Liu, J., Jeppesen, E., Zhu, G., Zhang, Y., Xu, H., Shi, K., and Deng, J.: Why Lake Taihu continues to be plagued with cyanobacterial blooms through 10 years (2007–2017) efforts, Sci. Bull., 64, 354–356, https://doi.org/10.1016/j.scib.2019.02.008, 2019.

Read, K. A., Lewis, A. C., Bauguitte, S., Rankin, A. M., Salmon, R. A., Wolff, E. W., Saiz-Lopez, A., Bloss, W. J., Heard, D. E., Lee, J. D., and Plane, J. M. C.: DMS and MSA measurements in the Antarctic Boundary Layer: impact of BrO on MSA production, Atmos. Chem. Phys., 8, 2985–2997, https://doi.org/10.5194/acp-8-2985-2008, 2008.

Revell, L. E., Edkins, N. J., Venugopal, A. U., Bhatti, Y. A., Kozyniak, K. M., Davy, P. K., Kuschel, G., Somervell, E., Hardacre, C., and Coulson, G.: Marine aerosol in Aotearoa New Zealand: implications for air quality, climate change and public health, J. R. Soc. N. Zealand, ahead-of-print, 1–23, https://doi.org/10.1080/03036758.2024.2319753, 2024.

Rocco, M., Dunne, E., Salignat, R., Saint-Macary, A., Peltola, M., Barthelmeß, T., Chamba, G., Barr, N., Safi, K., Marriner, A., Deppeler, S., Rose, C., Uitz, J., Harnwell, J., Engel, A., Colomb, A., Saiz-Lopez, A., Harvey, M. J., Law, C. S., and Sellegri, K.: Relating Dimethyl Sulphide and Methanethiol Fluxes to Surface Biota in the South-West Pacific Using Shipboard Air-Sea Interface Tanks, J. Geophys. Res.: Atmos., 130, https://doi.org/10.1029/2024jd041072, 2025.

Shen, J., Scholz, W., He, X.-C., Zhou, P., Marie, G., Wang, M., Marten, R., Surdu, M., Rörup, B., Baalbaki, R., Amorim, A., Ataei, F., Bell, D. M., Bertozzi, B., Brasseur, Z., Caudillo, L., Chen, D., Chu, B., Dada, L., Duplissy, J., Finkenzeller, H., Granzin, M., Guida, R., Heinritzi, M., Hofbauer, V., Iyer, S., Kemppainen, D., Kong, W., Krechmer, J. E., Kürten, A., Lamkaddam, H., Lee, C. P., Lopez, B., Mahfouz, N. G. A., Manninen, H. E., Massabò, D., Mauldin, R. L., Mentler, B., Müller, T., Pfeifer, J., Philippov, M., Piedehierro, A. A., Roldin, P., Schobesberger, S., Simon, M., Stolzenburg, D., Tham, Y. J., Tomé, A., Umo, N. S., Wang, D., Wang, Y., Weber, S. K., Welti, A., Jonge, R. W. de, Wu, Y., Zauner-Wieczorek, M., Zust, F., Baltensperger, U., Curtius, J., Flagan, R. C., Hansel, A., Möhler, O., Petäjä, T., Volkamer, R., Kulmala, M., Lehtipalo, K., Rissanen, M., Kirkby, J., El-Haddad, I., Bianchi, F., Sipilä, M., Donahue, N. M., and Worsnop, D. R.: High Gas-Phase Methanesulfonic Acid Production in the OH-Initiated Oxidation of Dimethyl Sulfide at Low Temperatures, Environ. Sci. Technol., 56, 13931–13944, https://doi.org/10.1021/acs.est.2c05154, 2022.

Smith, S. J., Aardenne, J. van, Klimont, Z., Andres, R. J., Volke, A., and Arias, S. D.: Anthropogenic sulfur dioxide emissions: 1850–2005, Atmos. Chem. Phys., 11, 1101–1116, https://doi.org/10.5194/acp-11-1101-2011, 2011.

Stark, H., Brown, S. S., Goldan, P. D., Aldener, M., Kuster, W. C., Jakoubek, R., Fehsenfeld, F. C., Meagher, J., Bates, T. S., and Ravishankara, A. R.: Influence of nitrate radical on the oxidation of dimethyl sulfide in a polluted marine environment, J. Geophys. Res.: Atmos., 112, https://doi.org/10.1029/2006jd007669, 2007.

Steinke, M., Hodapp, B., Subhan, R., Bell, T. G., and Martin-Creuzburg, D.: Flux of the biogenic volatiles isoprene and dimethyl sulfide from an oligotrophic lake, Sci. Rep., 8, 630, https://doi.org/10.1038/s41598-017-18923-5, 2018.

Tahan, A. and Shiroudi, A.: Oxidation reaction mechanism and kinetics between OH radicals and alkyl-substituted aliphatic thiols: H-abstraction pathways, Prog. React. Kinet. Mech., 45, 1468678319886129, https://doi.org/10.1177/1468678319886129, 2020.

Visscher, P. T., Kiene, R. P., and Taylor, B. F.: Demethylation and cleavage of dimethylsulfoniopropionate in marine intertidal sediments, FEMS Microbiol. Ecol., 14, 179–189, https://doi.org/10.1111/j.1574-6941.1994.tb00104.x, 1994.

Wang, C., Xu, D., Bai, L., Zhu, B., Huang, L., and Jiang, H.: Effects of accumulated cyanobacterial bloom biomass contents on the characteristics of surface fluid sediments in a eutrophic shallow lake, J. Environ. Manag., 308, 114644, https://doi.org/10.1016/j.jenvman.2022.114644, 2022.

Wang, H., Zhang, Y., and Mu, Y.: Rate Constants for Reactions of •OH with Several Reduced Sulfur Compounds Determined by Relative Rate Constant Method, Acta Phys.-Chim. Sin., 24, 945–950, https://doi.org/10.1016/s1872-1508(08)60041-8, 2008.

Wang, J., Xu, G., Chen, L., and Chen, K.: Atmospheric Particle Number Concentrations and New Particle Formation over the Southern Ocean and Antarctica: A Critical Review, Atmosphere, 14, 402, https://doi.org/10.3390/atmos14020402, 2023a.

Wang, J., Chu, Y.-X., Tian, G., and He, R.: Estimation of sulfur fate and contribution to VSC emissions from lakes during algae decay, Sci. Total Environ., 856, 159193, https://doi.org/10.1016/j.scitotenv.2022.159193, 2023b.

Wang, J., Wei, Z.-P., Chu, Y.-X., Tian, G., and He, R.: Eutrophication levels increase sulfur biotransformation and emissions from sediments of Lake Taihu, Sci. Total Environ., 887, 164054, https://doi.org/10.1016/j.scitotenv.2023.164054, 2023c.

Wang, K., Ge, M., and Wang, W.: Temperature dependent kinetics of the gas-phase reaction of OH radicals with EMS, Chin. Sci. Bull., 56, 391–396, https://doi.org/10.1007/s11434-010-4313-y, 2011.

Wang, M., Xu, X., Wu, Z., Zhang, X., Sun, P., Wen, Y., Wang, Z., Lu, X., Zhang, W., Wang, X., and Tong, Y.: Seasonal Pattern of Nutrient Limitation in a Eutrophic Lake and Quantitative Analysis of the Impacts from Internal Nutrient Cycling, Environ. Sci. Technol., 53, 13675–13686, https://doi.org/10.1021/acs.est.9b04266, 2019.

Wang, Y., Mehra, A., Krechmer, J. E., Yang, G., Hu, X., Lu, Y., Lambe, A., Canagaratna, M., Chen, J., Worsnop, D., Coe, H., and Wang, L.: Oxygenated products formed from OH-initiated reactions of trimethylbenzene: Autoxidation and accretion, Atmos. Chem. Phys. Discuss., 2020, 1–32, https://doi.org/10.5194/acp-2020-165, 2020.

Wine, P. H., Kreutter, N. M., Gump, C. A., and Ravishankara, A. R.: Kinetics of hydroxyl radical reactions with the atmospheric sulfur compounds hydrogen sulfide, methanethiol, ethanethiol, and dimethyl disulfide, J. Phys. Chem., 85, 2660–2665, https://doi.org/10.1021/j150618a019, 1981.

Wine, P. H., Thompson, R. J., and Semmes, D. H.: Kinetics of OH reactions with aliphatic thiols, Int. J. Chem. Kinet., 16, 1623–1636, https://doi.org/10.1002/kin.550161215, 1984.

Xu, H., McCarthy, M. J., Paerl, H. W., Brookes, J. D., Zhu, G., Hall, N. S., Qin, B., Zhang, Y., Zhu, M., Hampel, J. J., Newell, S. E., and Gardner, W. S.: Contributions of external nutrient loading and internal cycling to cyanobacterial bloom dynamics in Lake Taihu, China: Implications for nutrient management, Limnol. Oceanogr., 66, 1492–1509, https://doi.org/10.1002/lno.11700, 2021.

Ye, Q., Goss, M. B., Krechmer, J. E., Majluf, F., Zaytsev, A., Li, Y., Roscioli, J. R., Canagaratna, M., Keutsch, F. N., Heald, C. L., and Kroll, J. H.: Product distribution, kinetics, and aerosol formation from the OH oxidation of dimethyl sulfide under different RO2 regimes, Atmos. Chem. Phys., 22, 16003–16015, https://doi.org/10.5194/acp-22-16003-2022, 2022.

Yoch, D. C.: Dimethylsulfoniopropionate: Its Sources, Role in the Marine Food Web, and Biological Degradation to Dimethylsulfide, Appl. Environ. Microbiol., 68, 5804–5815, https://doi.org/10.1128/aem.68.12.5804-5815.2002, 2002.

Yu, C., Shi, C., Ji, M., Xu, X., Zhang, Z., Ma, J., and Wang, G.: Taste and odor compounds associated with aquatic plants in Taihu Lake: distribution and producing potential, Environ. Sci. Pollut. Res., 26, 34510–34520, https://doi.org/10.1007/s11356-019-06188-6, 2019a.

Yu, Y., Li, C., Shen, W., Wang, Z., Xu, P., and Yu, H.: Volatile compounds released by microalgae-water phase from Taihu Lake in China, Harmful Algae, 84, 56–63, https://doi.org/10.1016/j.hal.2019.01.009, 2019b.

Yvon, S. A. and Saltzman, E. S.: Atmospheric sulfur cycling in the tropical Pacific marine boundary layer (12°S, 135°W): A comparison of field data and model results: 2. Sulfur dioxide, J. Geophys. Res.: Atmos., 101, 6911–6918, https://doi.org/10.1029/95jd03355, 1996.

Yao, L., Garmash, O., Bianchi, F., Zheng, J., Yan, C., Kontkanen, J., Junninen, H., Mazon, S. B., Ehn, M., Paasonen, P., Sipilä, M., Wang, M., Wang, X., Xiao, S., Chen, H., Lu, Y., Zhang, B., Wang, D., Fu, Q., Geng, F., Li, L., Wang, H., Qiao, L., Yang, X., Chen, J., Kerminen, V.-M., Petäjä, T., Worsnop, D. R., Kulmala, M., and Wang, L.: Atmospheric new particle formation from sulfuric acid and amines in a Chinese megacity, Science, 361, 278–281, https://doi.org/10.1126/science.aao4839, 2018.

Zhao, Y., Schlundt, C., Booge, D., and Bange, H. W.: A decade of dimethyl sulfide (DMS), dimethylsulfoniopropionate (DMSP) and dimethyl sulfoxide (DMSO) measurements in the southwestern Baltic Sea, Biogeosciences, 18, 2161–2179, https://doi.org/10.5194/bg-18-2161-2021, 2021.

Zheng, B., Tong, D., Li, M., Liu, F., Hong, C., Geng, G., Li, H., Li, X., Peng, L., Qi, J., Yan, L., Zhang, Y., Zhao, H., Zheng, Y., He, K., and Zhang, Q.: Trends in China's anthropogenic emissions since 2010 as the consequence of clean air actions, Atmos. Chem. Phys., 18, 14095–14111, https://doi.org/10.5194/acp-18-14095-2018, 2018.

Zhou, C., Xu, X., Peng, Y., Wang, G., Liu, H., Jin, Q., Jia, R., Ma, J., Kinouchi, T., and Wang, G.: Response of sulfate concentration to eutrophication on spatio-temporal scale in freshwater lakes, Sci. Total Environ., 953, 176142, https://doi.org/10.1016/j.scitotenv.2024.176142, 2024.